Jernbaneverket

Statens vegvesen

Natural Hazards project: Work Package 6 - Quick clay

Characterization of historical quick clay landslides and input parameters for Q-Bing

39
2013

RAPPORT

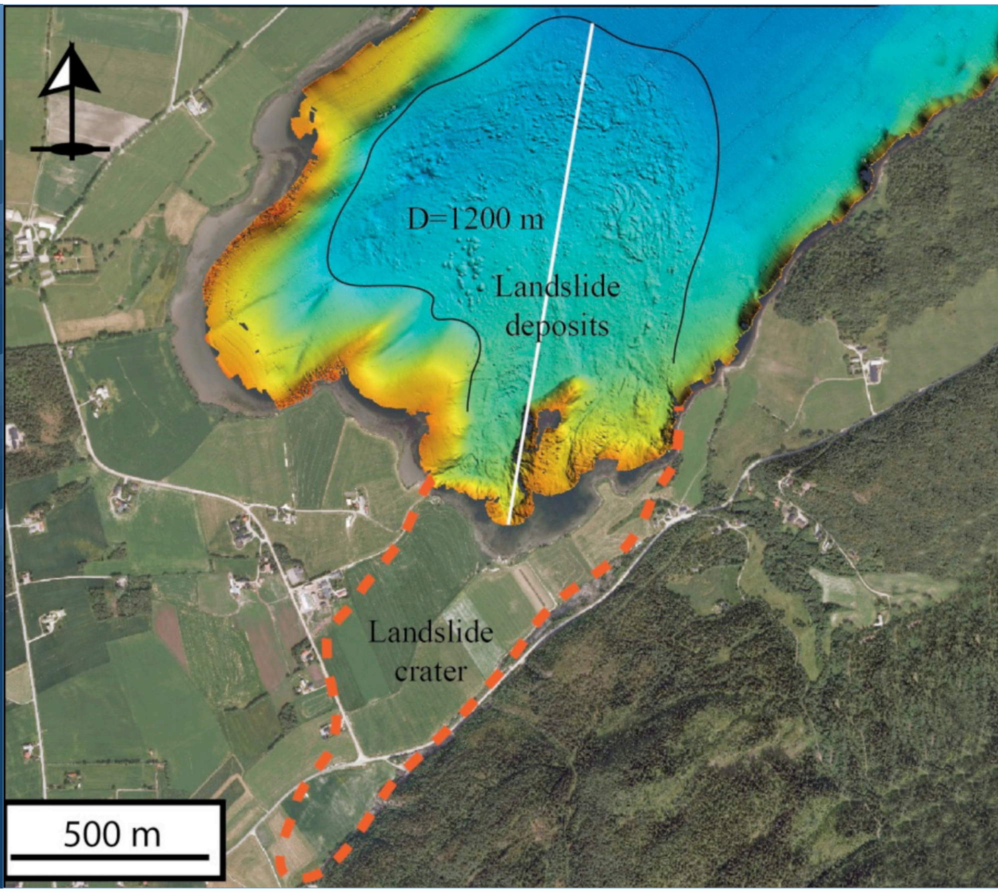

NIFS
NATURFARE
INFRASTRUKTUR - FLOM - SKRED

Natural Hazards project: Work Package 6 - Quick clay

Characterization of historical quick clay landslides and input parameters for Q-Bing

Norwegian Water Resources and Energy Directorate in collaboration with Norwegian Public Roads Administration and Norwegian National Railways Administration

2013

Report nr. 39/2013
Characterisation of historical quick clay landslides and input parameters for Q-Bing
Publisher: Norwegian Water Resources and Energy Directorate in collaboration with Norwegian Public Roads Administration and Norwegian National Railways Administration
Prepared by: Norwegian Geotechnical Institute (NGI)
Authors: Jean-Sebastien L'Heureux
Date: 27.12.2012
ISBN: 978-82-410-0908-2

Preface: Norwegian Public Roads Administration (NPRA), Norwegian Energy and Water Resources (NVE) and Norwegian National Railways Administration (NNRA) have initiated a National R&D project (2012-2015) called *Natural Hazards – Infrastructure for flood and slides.* The estimated budget for the project is 42 Million Norwegian Kroners. Quick clay is one of the seven work packages of the project. More information about the project can be obtained at www.naturfare.no

As a part of the on-going collaboration, NGI has been given a task to do a pre-study on the mobility of landslides in quick clays. The report presents an overview over landslides in Norwegian quick clays and input parameters necessary for the estimation of run-out distance using Q-Bing.

Keywords: Quick clay landslides, Q-Bing

NGI Rapport / Report

Q-Bing – Utløpsmodell for kvikkleireskred

Characterization of historical quick clay landslides and input parameters for Q-Bing

20120753-02-R
17 January 2013
Revision: 0

Main office:
PO Box 3930 Ullevål Stadion
NO-0806 Oslo
Norway

Trondheim office:
PO Box 1230 Sluppen
NO-7462 Trondheim
Norway

T (+47) 22 02 30 00
F (+47) 22 23 04 48

BIC No. DNBANOKK
IBAN NO26 5096 0501 281
Company No.
958 254 318 MVA

ngi@ngi.no
www.ngi.no

Project

Project title:	Q-Bing – Utløpsmodell for kvikkleireskred
Document title:	Characterization of historical quick clay landslides and input parameters for Q-Bing
Document No.:	20120753-02-R
Date:	17 January 2013
Revision/Rev. date:	0

Client

Client:	Statens Vegvesen, Vegdirektoratet
Client's contact person:	Vikas Thakur
Contract reference:	Contract, revised 2012-08-20

For NGI

Project manager:	Dieter Issler
Prepared by:	Jean-Sebastien L'Heureux
Reviewed by:	Kjell Karlsrud and Dieter Issler

Summary

The post-failure mechanism associated to Norwegian quick clay landslides is a complex natural phenomenon. An attempt is made in the present study to characterize the mobility of such landslides on the basis of well-documented cases and available relationships from laboratory data. Factors affecting mobilization into flows and run-out distances are discussed. During a landslide the flow behavior can be quite complex and various types of flow behavior can exist depending on the clay type, sensitivity, remoulded shear strength, pore-water salinity, mineralogy, and water content. Results show that the remoulded shear strength in soil mechanics is similar to values of yield strength in rheology. There is, however, a large discrepancy between values of viscosity determined empirically from laboratory data and those obtained from back-calculation of landslide events. Hence, there is a need for field and laboratory calibration of these models.

Contents

1 Introduction

Landslides are common in the sensitive marine clay deposits of Canada and Scandinavia. In Norway, at least 1150 people died in historical time as a consequence of such landslides (Furseth 2006). The 1345 landslide and following flood in the Gaula valley is the largest event recorded in Norway with over 500 victims (Rokoengen et al. 2001). The quick-clay landslide in Verdal, where a total of 116 people perished in 1893, is also well documented (e.g. Walberg 1993).

Following the famous Rissa landslide in mid Norway (Gregersen 1981, L'Heureux et al. 2012), a nationwide quick-clay mapping program was started in order to delimitate areas susceptible to large quick-clay landslides. Until today, the produced susceptibility and hazard maps have been restricted to identifying potential release areas for large landslides without regard to the post-failure mechanisms of the debris (e.g. run-out distance). Due to the increasing societal awareness, the need for mapping the potential run-out areas has been increasingly felt in recent times. However, the flow behavior of quick clay landslides is complex and there are only a few studies documenting the mobility of landslides in sensitive clays (Edgers &Karlsrud 1982, Locat et al. 1992, Locat et al. 2003, Locat et al. 2008). One of the main problems is that landslide debris is often difficult to map following an event because it tends to end up in streams, rivers or in near-shore environments.

In order to develop a suitable tool for calculating the run-out distances of quick clay landslides (i.e. Q-Bing code), a thorough study of historical events is needed. For this reason, an inventory of Norwegian landslides in sensitive clay has been prepared based on the work by Natterøy (2011), L'Heureux (2012) and L'Heureux and Solberg (2012). The first two sections of this report focus on the characteristics of Norwegian clays and the type of landslides generally observed in this material. Thereafter, the morphological and geotechnical data for 39 landslides in sensitive clay in Norway is presented. These data offer a unique possibility to study the mobility of quick clay landslides and to estimate flow properties and rheological parameters as input for the numerical model. The mechanisms of importance for mobilization into flows (i.e. transformation from intact to remoulded conditions) are also discussed based on laboratory data and field observations.

2 Characteristics of Norwegian quick clay

2.1 Definition

In Norway, the classification of a clay material as quick is based upon the sensitivity of the soil (i.e. the ratio between the undrained shear strength s_u and the remoulded shear strength s_{ur}) and a threshold value of the remoulded shear strength. Clays are classified as quick when the remoulded shear strength is less than 0.5 kPa and the sensitivity (S_t) is greater than 30 (NGF 1974). More recently, the Norwegian Water and Energy Directorate (NVE) published guidelines recommending the use of $S_t \geq 15$ and $s_{ur} \leq 2$ kPa for brittle clay material which would collapse during a landslide (NVE 2009).

2.2 Formation and origin

Sensitive clay materials are found in several areas of the world including Alaska, Canada, Norway and Sweden. In Norway, the quick clays generally occur in marine clay deposits found in the low-land areas of the country. The distribution of such deposits is closely linked to the postglacial and Holocene landscape development. During the last ice-age, large portions of the country were depressed under the weight of the Fennoscandian ice-sheet which covered most of the land. Glacial scour removed most of the pre-glacial deposits and covered the rock floor and valley sides with an irregular layer of moraine, in places also overlain by glacio-fluvial material. With the retreat of the ice-fronts and establishment of saline fjord conditions, large quantities of finer fractions were washed out from the glacial deposits, transported by rivers and redeposited in the fjords to form late glacial marine deposits. The clay particles have a tendency to flocculate when deposited in saline fjord and sea waters, leading to an open “card house” structure in the marine clay deposits.

The isostatic uplift that followed the ice retreat led to the emergence of the marine deposits during the last 10,000 years. With time, the flux of fresh groundwater through the clay deposits has led to leaching of the salts within the grain structure of the material. Such leaching takes a long time (i.e. hundreds to thousands of years) since the permeability of clay material is low. Nevertheless, in some areas, the leaching process is accelerated because of specific geological and topographical conditions that increase the groundwater flow (e.g. near the bedrock and clay interface, in slopes where the hydraulic gradient is higher, in zones where the clay deposit is inter-bedded with coarser material (silt/sand/gravel) (Figure 1).

The high sensitivity of Norwegian quick clays is attributed to the leaching, by fresh groundwater, of the salts within the grain structure (Rosenqvist 1953). Removal of salt ions in the pores to values of about 2–5 g/l can result in a metastable sensitive clay structure. Upon remoulding, this unstable structure is destroyed and the inter-particle surface water that is liberated gives rise to a liquid type fluid (Rosenqvist 1966). This potential to liquefy when subjected to loading is one of the main agents governing the post-failure behavior of quick clays.

Quick clay is however not a final stage of development. With further leaching the groundwater may add stabilizing ions to the clay structure, thus leading to a new stable clay fabric. Such a process is generally encountered in the first few meters below the surface where a dry crust may form above the groundwater level and the sensitive clay material.

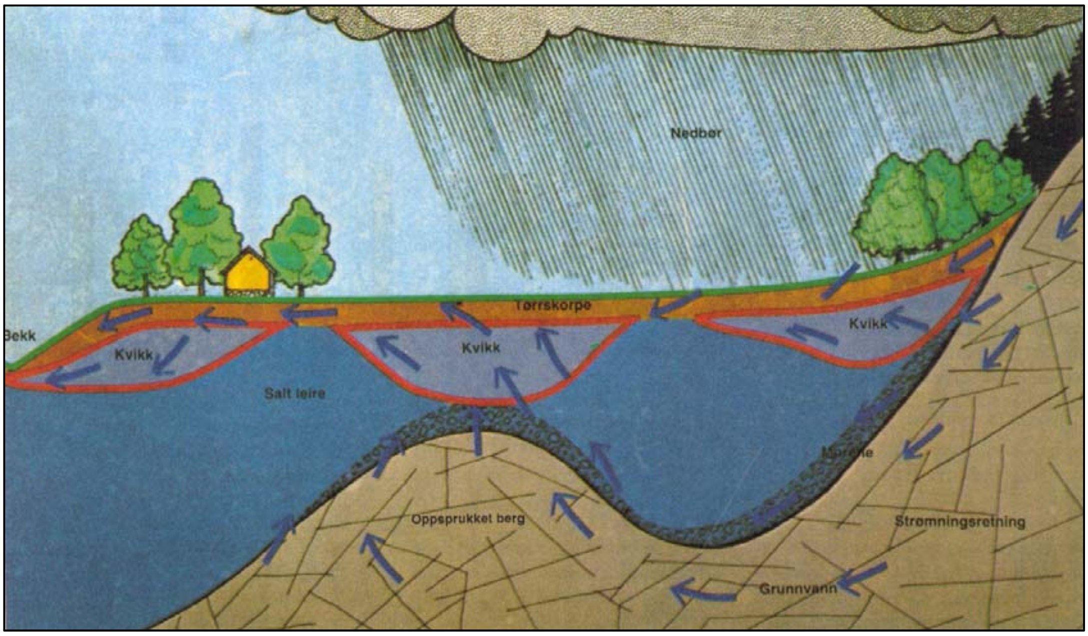

Figure 1: Conceptual model showing zones where quick clay is often found (Løken 1983).

3 Types of landslides in sensitive clays

According to Tavenas (1984) and Karlsrud et al. (1984), four main types of landslides can generally be observed in the sensitive clays of Canada and Scandinavia: single rotational slides; multiple retrogressive slides (sometimes described as earthflows or flows); translational progressive landslides; and spreads (Figure 2). The last three types occur very suddenly and often cover large areas. Translational progressive landslides are uncommon in eastern Canada, but are often observed in Scandinavia (e.g. Aas 1981, Karlsrud et al. 1984). On the other hand, spreads represent about 42% of the large landslides in eastern Canada clays (Locat et al. 2011), the rest being generally flows or unidentified retrogressive landslides. As observed by Karlsrud et al. (1984), a combination of the four types of landslides can often be observed in one event. The Mink Creek landslide in British-Columbia (Geertsema et al. 2006) is a good example where flow and spread occurred successively in one landslide event. The Rissa landslide in Norway is also a good example where several types of landslides (initial slide, flake type and flow) were involved; (Gregersen 1981).

Among the large landslides occurring in sensitive clays, flows are well described and the most common in Norway (Bjerrum 1955; Tavenas 1984). Multiple retrogressive slides are believed to result from an initial failure, the debris of which becomes strongly remoulded and flows out of the crater, leaving an unstable scarp. A second slide may then occur with the remoulded clay also flowing out of the crater, generating another unstable scarp. This process can continue until a final stable backscarp is formed and the retrogression stops (Figure 2a). This type of landslide is characterized by an empty crater (minimal debris is left in the crater after the movement) having in some cases a bottle-neck shape. Multiple retrogressive slides tend to occur when: (a) the potential energy in the slope is high enough to remould the clay effectively, (b) the remoulded clay is liquid enough to flow out of the landslide crater [i.e. liquidity index higher than 1.2 or remoulded shear strength lower than 1 kPa; Lebuis et al. (1983), L'Heureux et al. (2012)] and (c) the topography enables evacuation of the debris. A typical example of this type of landslide in Norway is the Ullensaker slide in 1953 (Bjerrum 1955).

Translational landslides result from the development of a shear surface parallel to the ground surface, above which the soil mass displaces downhill (Cruden and Varnes 1996). Translational progressive landslides are characterized by a zone of subsidence at the head of the slope and an extensive compressive heave zone located far beyond the toe of the slope, in more horizontal ground (Figure 2b). Such landslides are also often referred to as flake-type landslides in Norway. An example is the Bekkelaget landslide, which occurred in 1950 (Eide & Bjerrum, 1955).

According to Cruden and Varnes (1996), spreads result from the extension and dislocation of the soil mass above the failure surface, forming horsts and grabens that subside in the underlying remoulded material forming the shear zone. Horsts are blocks of more-or-less intact clay, often with a sharp wedge pointing upward, and grabens are blocks having typically a flat, horizontal top surface (Figure 2c). Those geomorphologic shapes are key elements distinguishing spreads from other retrogressive landslides. The perfect example of a spread in sensitive clay material is the 2010 landslide at St-Jude, Quebec, Canada (Locat et al. 2011).

Presentation of field data in Table 1 presents an overview of some landslides in sensitive clay soils from Norway. The catalogue builds on studies performed by Natterøy (2011), L'Heureux (2012) and L'Heureux and Solberg (2012). The geomorphological parameters collected for each landslide were estimated based on topographical and/or bathymetrical maps available prior to and after the landslides with a vertical resolution of the contour lines better than 1 m . In the cases were no information was available before the landslide occurred (e.g. pre-historic events), the parameters were estimated based upon the surrounding terrain morphology.

Mobilized landslide volumes were estimated by multiplying the area of the failure zone with the average depth of the landslide crater. The run-out distances were estimated both from the outlet of the landslide (D) and from the backscarp (D_t), (Figure 3). Estimating the thickness of the landslide debris (H_D) is not an easy task as ground thruth is seldom available. For landslides that deposited in the fjords, good estimates can be made based on geophysical data (e.g. seismic reflection profiles). In other cases, the best estimates rely on data from the literature and terrain analysis. Index properties and geotechnical information for most of the landslides were obtained from literature data and geotechnical reports (Table 2). For a few of the landslides, mass flow velocity was estimated based on witness observations and video recording (e.g. Rissa landslide) (Table 3).

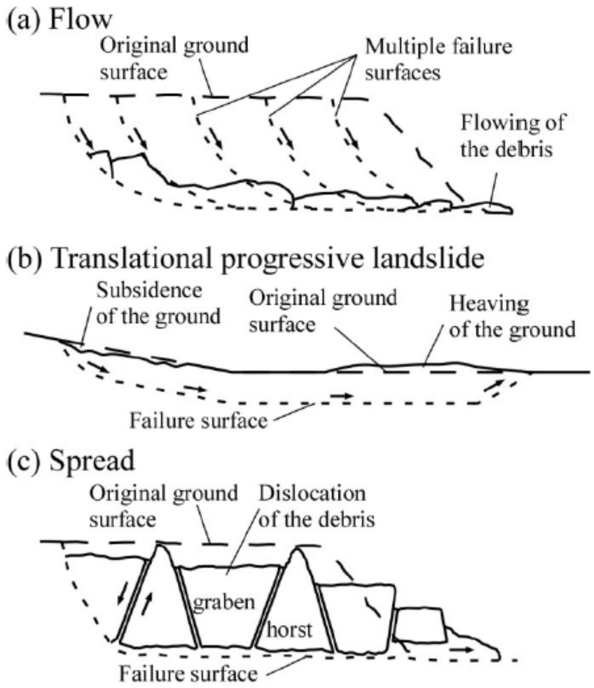

Figure 2: Types of landslides in sensitive clays: a) multiple retrogressive landslide or flow, b) translational progressive landslide or flake, and c) spread (from Locat 2012).

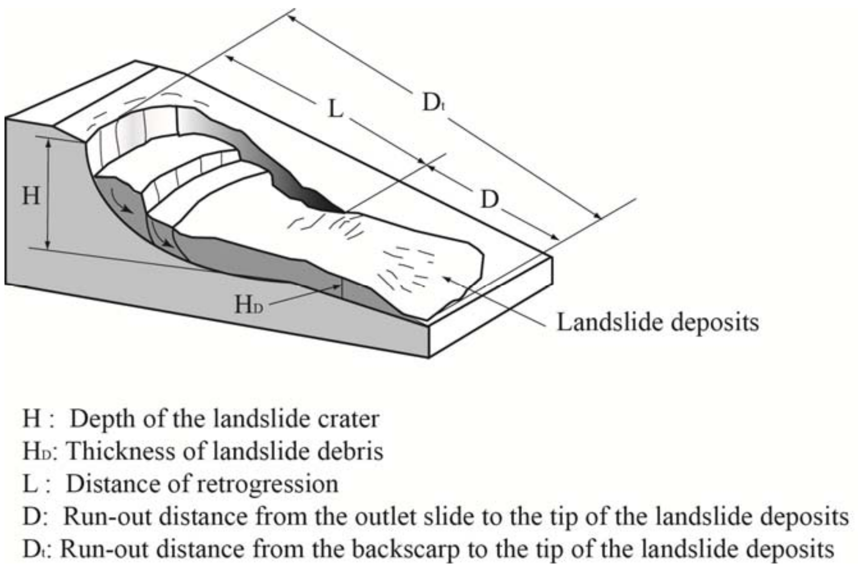

Figure 3: Conceptual landslide model showing some of the morphological parameters compiled in this study (after L'Heureux 2012).

Table 1: Overview of landslides in Norwegian clays (adapted from L'Heureux 2012).

No	Location	Date	Type of landslide	Volume (m^3)	$W_{avg.}$	L (m)	D (m)	H_D (m)	Reference
1	Bakklandet	10.11.1634	Flow	500 000	130	75			Bjerrum & Kjærnsli (1957)
2	Bekkelaget	07.10.1953	Flake	100 000	160	165	20		Eide & Bjerrum (1955)
3	Brå	01.05.1928	Flake	500 000	500	200	400	20?	Holmsen (1929)
4	Byneset	01.01.2012	Flow	350 000	100	400	900	3	NVE files, Thakur (2012)
5	Båstad	05.12.1974	Spread	1 500 000	450	325	700	3	Gregersen & Løken (1979)
6	Drammen	06.01.1955	Spread	4 000	50	45			Bjerrum & Kjærnsli (1957)
7	Døla	19.06.2011	Spread	30 000	50	65	30		NGI (2011)
8	Hyggen	23.01.1978	Flow	500 000	100	40	450		Karlsrud (1979), Hansen et al. (2011)
9	Duedalen	18.07.1625	Flow	500 000	195	380			L'Heureux (2012)
10	Fallet, Rissa	1997	Flow	200 000	130	150	670		L'Heureux et al. (2011)
11	Finneidfjord	20.06.1996	Flow	1 000 000	300	150	1000	1.4	Longva et al. (2003)
12	Fredrikstad	17.08.1980	Spread	10 000	25	50	30		Karlsrud (1983)
13	Furre	14.04.1959	Flake/Spread	3 000 000	720	400	0-90		Kenney (1967)
14	Gretnes	17.04.1925	Flow	400 000	220	210			Holmsen (1929)
15	Gullaug 1	29.11.1974	Flow	100 000	190	40	325		Karlsrud (1979), Hansen et al. (2011),
16	Gullaug 2	Pre-historical	Flow	100 000	380	500			L'Heureux (2012)
17	Heimstad	Pre-historical	Flow	900 000	220	370			L'Heureux (2012)
18	Hekseberg	20.03.1967	Flake	200 000	150	160	300		Drury (1968)
19	Kattmarka	13.03.2009	Spread and flow	600 000	80	300			Nordal et al. (2009)

Table 1 (continued)

No	Location	Date	Type of landslide	Volume (m^3)	W_{avg}	L (m)	D (m)	H_D(m)	Reference
20	Kokstad	21.10.1924	Spread and flow	400 000	180	180	600		Holmsen (1929)
21	Lade	11.04.1944	Spread	50 000	210	25	100		Holmsen & Holmsen (1946)
22	Langørjan	Pre-historical	?	11 000 000	1000	500			L'Heureux (2012)
23	Leirfossen	Pre-historical	?	75 000 000	1200	3500			L'Heureux (2012)
24	Lodalen, Oslo	06.10.1954	Spread	10 000	50	40			Sevaldson (1956)
25	Lund	Pre-historical	Flow	4 600 000	500	1050			L'Heureux (2012)
26	Lyngseidet	03.09.2010	Flow	220 000	120	160	420		L'Heureux (2012)
27	Olderdalen	Pre-historical	Flow	25 000 000	450	1600			L'Heureux (2012)
28	Othilienborg	Pre-historical	Flow	70 000 000	1000	1700	11000		L'Heureux et al. (2009)
29	Rissa (initial)	29.04.1978	Flow	150 000	80	450	620		L'Heureux et al. 2012
30	Rissa (main)	29.04.1978	Flake and Flow	5 000 000	400	1400	1200	6	Gregersen (1981), L'Heureux et al. 2012
31	Rørdal	Pre-historical	?	3 300 000	270	890			L'Heureux (2012)
32	Selnes	18.04.1965	Spread and flow	140 000	166	215	400	2	Kenney (1967)
33	Skjelstadmarka	14.08.1962	Flow	2 000 000	200	600	2240		Trak & Lacasse (1996)
34	Sjetnemarka	Pre-historical	Flow	30 000 000	1100	1050			L'Heureux (2012)
35	Stavset	Pre-historical	Flow	800 000	200	125			L'Heureux (2012)
36	Tiller	07.03.1816	Flow	550 000	610	350			L'Heureux (2012)
37	Ullensaker	23.12.1953	Flow	200 000	180	195	1500	4	Bjerrum (1955)
38	Verdal	19.05.1893	Flow	65 000 000	1000	2000	9000		Trak & Lacasse (1996)
39	Vibstad	22.02.1959	Spread	1 400 000	325	250	250		Bjerrum (1955)

Table 2: Index properties and geotechnical parameters for some of the landslides presented in Table 1.

No	**Location**	**γ (kN/m3)**	**s_u (kPa)**	**Max S_t**	**s_{ur} (kPa)**	**I_P**	**I_L**
1	Bakklandet	18.9	10–19	210	0.07	7	1.8
2	Bekkelaget	18.9	10	80	0.13	9	2.4
3	Brå	19.0	18	75	0.24	5.5	2
4	Byneset	18.3	10–25	113	0.20	5	4.2
5	Båstad	19.3	30–40	100	0.65	6	1.6
6	Drammen	19.1	20	4	2.00	14.2	0.8
7	Døla	20.0	12	40	0.3	7.7	1.8
8	Hyggen	19.0	10	20	2.00	-	0.5
9	Duedalen	18.9	10–19	210	0.07	4	4.0
10	Fallet, Rissa	18.4	15–20	12	0.8	5	1.2
11	Finneidfjord	18.8	7–10	100	0.08	6.00	2.5
12	Fredrikstad	19.0	15	20	0.9	20	1
13	Furre	19.0	35–45	30	0.67	10	2.3
15	Gullaug 1	19.0	12	4	3.00	10	1
18	Hekseberg	19.0	20–30	150	0.17	7	3.2
19	Kattmarka	19.0	15	60	0.25	6	3
21	Lade	19.2	20–30	16	1.56	10	1.00
24	Lodalen, Oslo	19.1	45	3	15	18	0.72
26	Lyngseidet	19.2	5	52	0.15	7	2.4
27	Olderdalen	20.0	20–30	70	0.43	4	3
28	Othilienborg	19.3	10–25	83	0.30	4	4.2
29	Rissa 1	18.6	10–20	100	0.24	10	2.3
30	Rissa 2	18.6	10–20	100	0.24	5	2.3
32	Selnes	18.6	15–20	100	0.17	6	1.9
33	Sjetnemarka	20.0	23	86	0.27	4.5	2.2
34	Skjelstadmarka	19.3	40	48	0.83	6	1.6
36	Tiller	18.7	20–40	150	0.20	4	2.0
37	Ullensaker	18.6	10–25	42	0.43	7	1.2
38	Verdal	19.3	10–200	40	0.20	4	2.5
39	Vibstad	18.3	30–70	40	1.25	7	1.3

Table 3: Maximum observed velocity of quick clay landslides. All landslides are from Norway with the exception of the St-Jean-Vianney landslide, which occurred in eastern Canada.

Landslide	Maximum velocity (m/s)	Comments	Reference
Båstad, Trøgstad	< 1	Low velocity	Gregersen and Løken (1979)
Bekkelaget	1-2	The landslide happened very quickly. The most substantial movement occurred within less than half-a-minute; possibly 15-20 seconds. Rotational/spread movement without flow!	Eide and Bjerrum (1954)
Rissa	11.3	From amateur video. In the initial phase, the large flake of clay moved at a speed of 2.7–5.5 m/s (10–20 km/h) and the velocity increased in the later phase of the landslide up to 8.3–11.3 m/s (30–40 km/h). Results from modeling with BING suggest that the maximum velocity occurred off the steep shoreline slope in Lake Botn (up to 18 m/s).	Gregersen (1981), L'Heureux et al. (2012)
Verdal	15	v = 10-15 m/s out of the pit and $v \sim 1.7$ m/s in the lower parts	Karlsrud and By (1981)
St-Jean-Vianney, Canada	7.2		Tavenas et al. (1971)

4 Retrogression and run-out distances for Norwegian landslides

In considering the mobility of a landslide, one can distinguish between two components (Figure 3): the retrogression (L) and the run-out distance (D). For landslide in sensitive clays, the ability of the clay to be remoulded is of great importance. This process depends on the mechanical properties of the clay and on the available potential energy (i.e. the height of the slope). Because of this, the distance of retrogression has previously been related to the stability number ($N_s = \gamma H/s_u$) (Mitchell and Markell 1974, Trak and Lacasse 1996). Such a relationship is presented in Figure 4 for the Norwegian landslides. Similar to the work by Mitchell & Markell (1974), the data shows an increase in the distance of retrogression with the stability number although other factors such as sensitivity, stratigraphy and topography also play a significant role in limiting retrogression. The stability number for the landslides at Lyngseidet and Sjetnemarka, for example, indicate that the length of retrogression should have been higher for these events (Figure 3). Geotechnical soil profiles in both cases show a strong decrease in sensitivity upslope, which probably governed part of the retrogressive process (see also L'Heureux and Solberg 2012).

Another important factor contributing to the mobility of the landslides in sensitive clays is the ability of the clay to flow out of the landslide crater when remoulded.

This depends on the consistency of the remoulded material and on the liquidity index. Results in Figure 5 show that flow slides generally occur when I_L > 1.1–1.2 and the sensitivity is greater than 30. Such results are similar to those obtained by Lebuis et al. (1983) for landslides in eastern Canada. Of particular interest here is the 2011 landslide at Døla near Mosjøen which remained mostly as limited deformation. The value of I_L taken is not representative for the whole deposit at Døla since the thin quick clay layer here (i.e. 1–2 m) is covered by more than 5 m of sand and gravel (see further discussions in Chap. 6).

In Figure 6 the data suggests that the magnitude of retrogression is governed to a large extent by the capacity of the remoulded landslide debris to flow out of the landslide crater. The upper trend is well described by $D \sim 10\ L$ for the Norwegian landslide. Factors affecting this outflow will therefore play an important role in the development of retrogression and vice-versa (e.g. remoulded strength of the clay, sensitivity of the deposit and morphology of the slide scar). The topography of the valley in the vicinity of the slide is particularly important. Therefore, large retrogressions and long run-out distances are more likely to occur in valleys with steep longitudinal gradients or near wide and deep rivers or lakes than in flat, narrow valleys. This is illustrated in Figures 8 and 9 for the Rissa and the Finneidfjord landslides, respectively. In both these cases, the fjord bottom permitted the evacuation of the debris, which facilitated retrogression.

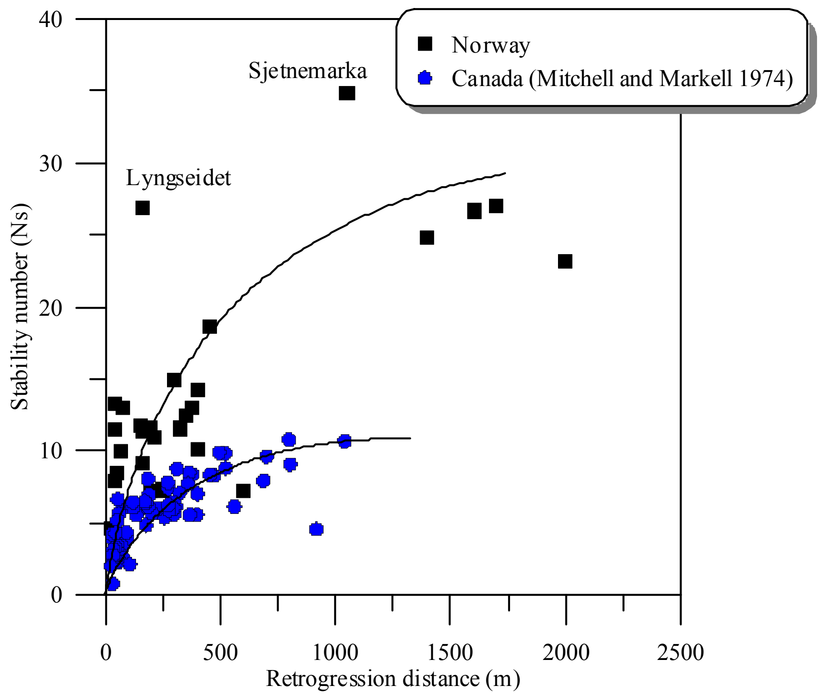

Figure 4: Stability number versus retrogression distance for Canadian and Norwegian landslides in sensitive clays.

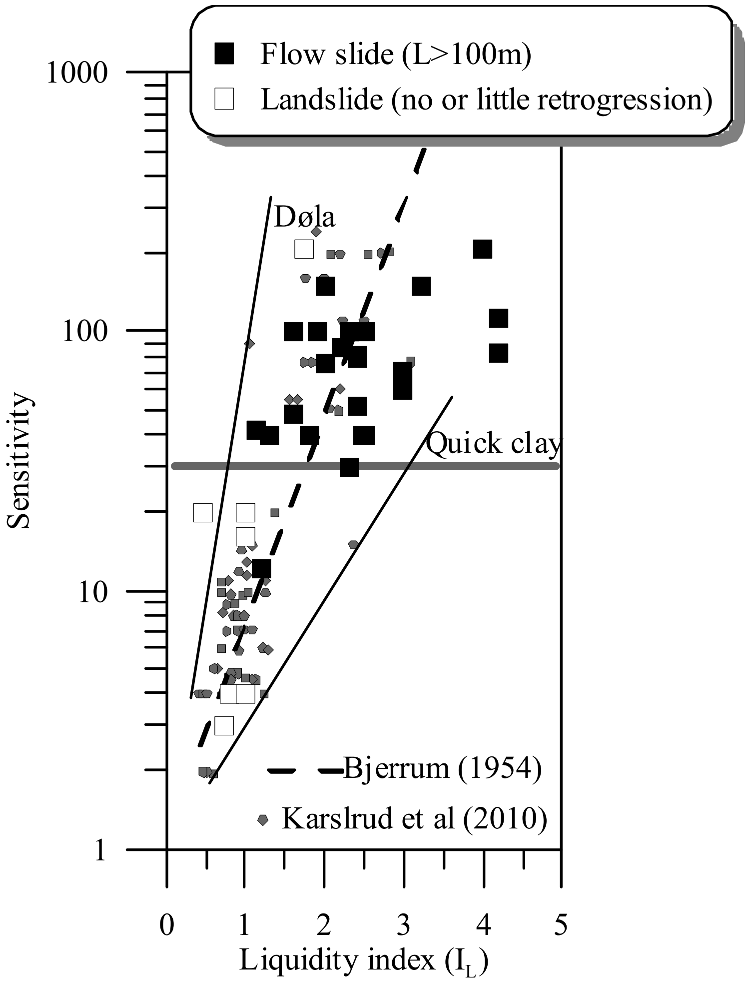

Figure 5: Liquidity index plotted against sensitivity for quick clay landslides observed in Norway.

Similarly to the work performed by Edgers & Karlsrud (1982) and Locat et al. (2008), Figure 7 shows that the run-out distance for Norwegian quick clays generally increases with the volume of failed sediment (Vol) per unit width (W_{avg}). This ratio actually represents the longitudinal section (A) of the landslides. Results from Figure 6 and 7 also show that for a given Vol/W_{avg}, the run-out distances for the Norwegian landslides is greater than for those in eastern Canada. The upper trend for the Norwegian cases is given by

(1) $$D = 9 \cdot \left(\frac{Vol}{W_{avg}}\right)^{0.73}$$

whereas the upper bound for the Canadian landslides is given by:

(2) $$D = 1.3 \cdot \left(\frac{Vol}{W_{avg}}\right)^{0.73}$$

Such differences may be attributed to the physical and mechanical properties of the clay (i.e. the over-consolidation ratio (OCR), s_{ur}, I_L and I_p). Clays from eastern Canada are generally more over-consolidated and have a higher undrained strength in relation to vertical effective stress than those found in Norway. Karlsrud et al (1984) attributed this to cementation effects in the Canadian clays, not found in Norwegian clays. It would therefore be expected that it requires more energy to remould Canadian clays as compared to Norwegian clays. Another reason for the observed differences may lie in the type of environment in which these landslides occurred. For example, the inclusion of channelized flow events in the present study may lead to over-estimating the mobility of the Norwegian landslides (Figs. 6–7). Moreover, some quick-clay landslides in Norway occur in near-shore areas where the debris has the possibility to flow on a fjord bottom (e.g. Figs. 8–9). For such cases, the low permeability of the clays may ensure water entrapment below the landslide masses resulting in hydroplaning and longer run-out distances in the submarine environment (e.g. De Blasio et al. 2005).

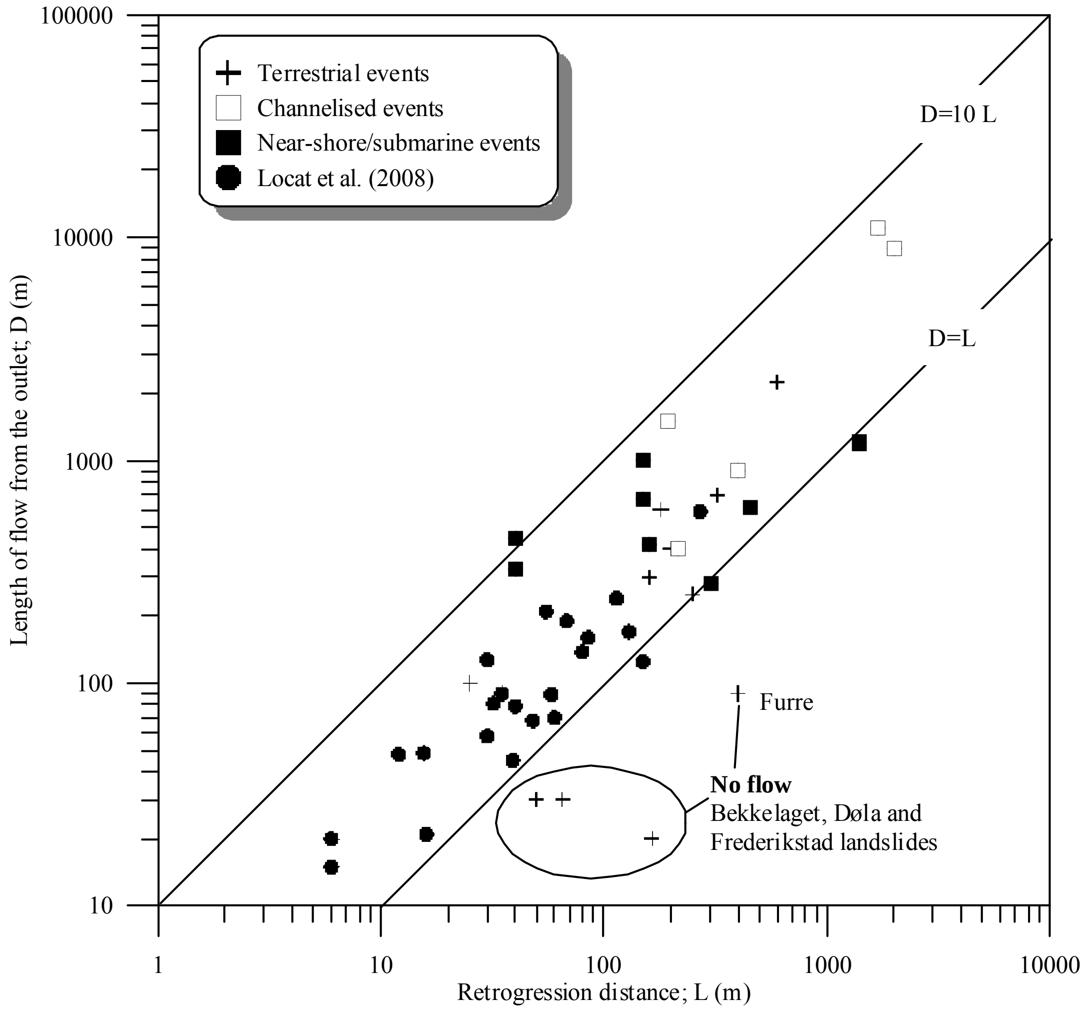

Figure 6: Mobility estimated for Norwegian quick clay landslide as a function of the retrogression distance (extended data set from (L'Heureux 2012)). The data is compared to landslides in sensitive clays from eastern Canada.

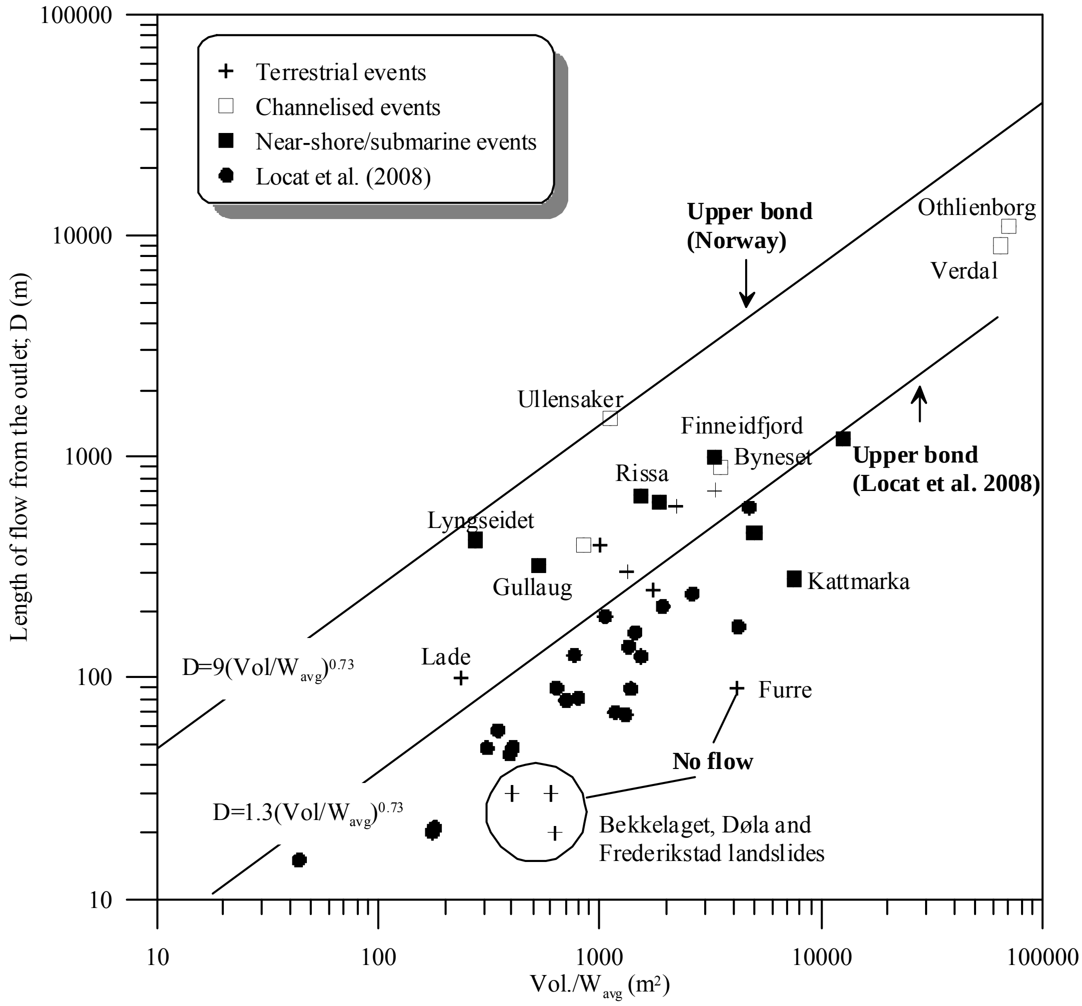

Figure 7: Mobility of Norwegian quick clay landslides as a function of the normalized volume of disturbed material per unit width (extended data set from (L'Heureux 2012)). The data is compared to landslides in sensitive clays from eastern Canada (Locat et al. 2008).

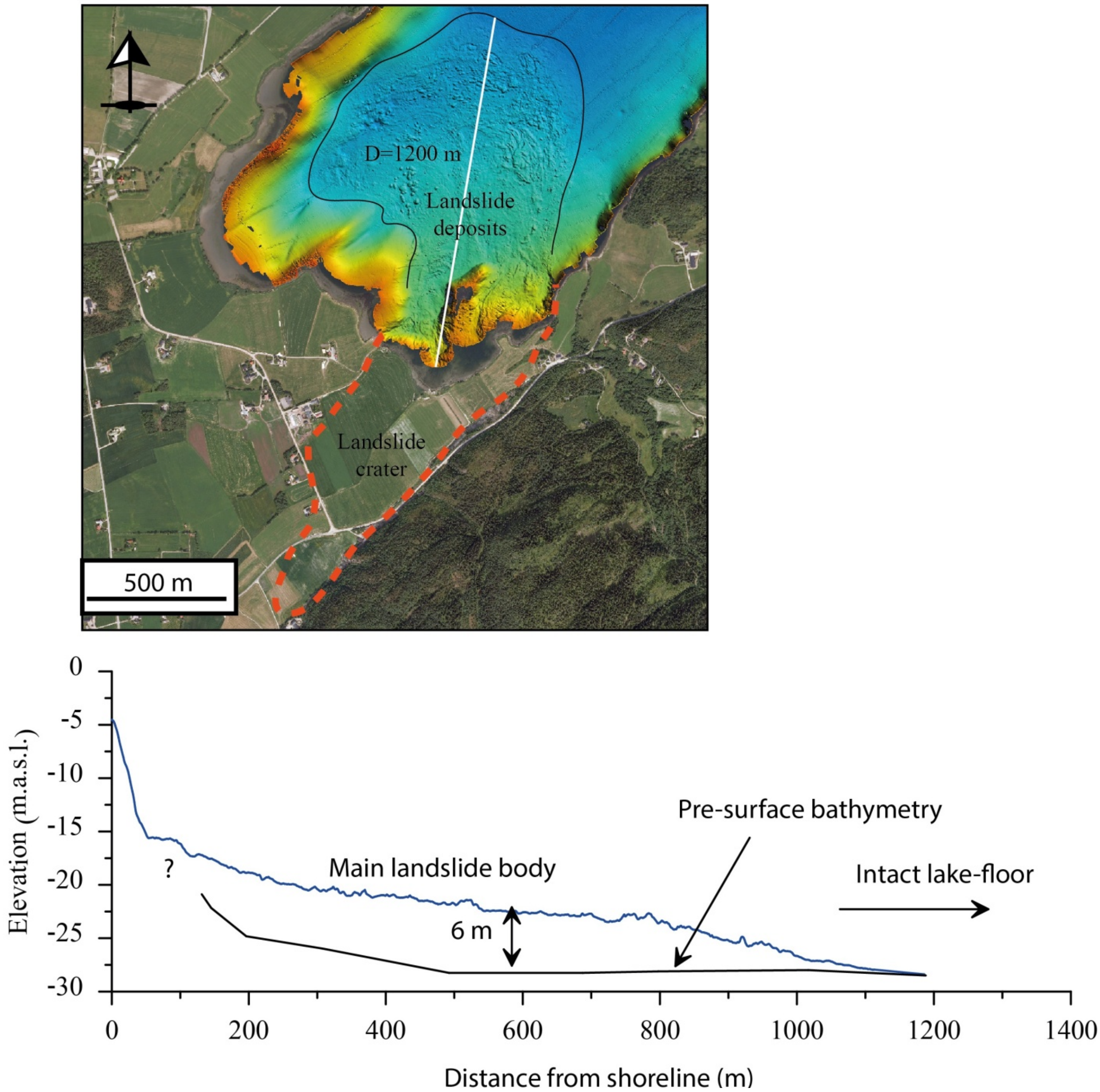

Figure 8: Rissa landslide with morphology of the debris mapped in Lake Botn and landslide crater on land. The lower panel presents a slope profile prior and after the 1978 landslide. The thickness of the landslide debris was evaluated using seismic reflection data in Lake Botn (data from L'Heureux et al. 2012).

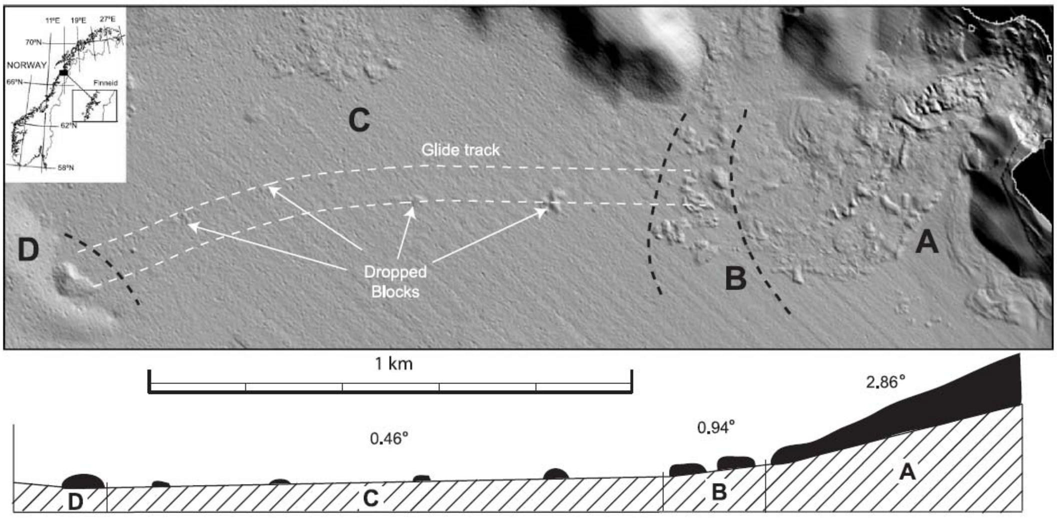

Figure 9: Finneidfjord landslide with slide morphology divided into zones. Zone A: Main lobe. Zone B: Zone with scattered blocks. Zone C: Glide zone. Zone D: Main outrunner block. Average bottom slopes along the slide and glide path are shown in the lower panel. (From Ilstad et al. 2004).

5 Passage from intact to remoulded soil conditions

Following initial failure, some landslides mobilize into flows, whereas others remain as limited deformation. In general, the mechanisms for mobilization into flows are not well understood. However, the long run-out distances observed for landslides in sensitive clays have previously been related to the low remoulded shear strength (or viscosity) of the soil following failure. The mobility of most flows in such material is acquired at the time of failure as some energy is available for remoulding. From this moment, the mobility of the soil will mostly depend on how this energy is distributed within the mass. The potential energy (E_p) of a soil mass can be written as:

(3) $$E_p = H_G \cdot \gamma \cdot V$$

where V is the volume of landslide, γ is the average unit weight of the soil and H_G is the vertical displacement of the center of gravity between the initial and final stage of the landslide. The total energy within the landslide at time t is defined as (Vaunat, 2002):

(4) $$\Delta E_T = \Delta E_p(t) + \Delta E_F(t) + \Delta E_R(t) + \Delta E_k(t) = 0$$

Parts of the energy will be dissipated in friction (E_F) while the rest will be used to remould the soil (E_R) and to accelerate the mass of debris until a certain velocity (kinetic energy; E_K). The debris will come to rest when the kinetic energy approaches zero (i.e. when all of the potential energy has been used for remoulding, internal deformation and friction). Remoulding occurs when the microstructure of the soil is destroyed or when the stress conditions have reached past the limit stress state. Fully remoulded conditions are reached when a constant and minimum value of undrained shear strength is acquired (i.e. remoulded shear strength s_{ur}).

Following Vaunat and Leroueil (2002) an estimation of the remoulding state can be given by using the destructuration index (I_D):

(5) $$I_D = \frac{E_P}{E_R}$$

For an I_D larger than unity, the potential energy in a given volume of clay would be larger than the energy needed to fully remould the clay. Such a situation should be observed at sites where flow slides have previously occurred.

In Sweden, Söderblom (1974) observed that clays with identical sensitivity values needed a different quantity of energy to reach a fully remoulded state. He used the term “rapidity” to describe this particularity. This author also proposed a qualitative scale of rapidity based on the damages observed on a clay sample with normalized dimension which was submitted to 250 strokes in the Casagrande apparatus. The scale ranges from 1 (no damages) to 10 (fully remoulded conditions). Callenday and Smiley (1984) showed that such experiments are not suitable for clays from eastern Canada as the test could not deliver enough energy for the clay to reach a remoulded state.

Flon (1982) and Tavenas et al. (1983) performed different tests to study the remoulding energy of clays: free-fall, impact from falling object, extrusion and simple shear. Simple shear was found to give the best results as the applied load and the loss of strength could be continuously followed. In order to follow the remoulding evolution these authors proposed using the remoulding index:

(6) $$I_R = \frac{s_u - s_{ux}}{s_u - s_{ur}}$$

where s_u is the undrained shear strength, s_{ur} is the remoulded shear strength and s_{ux} is the remoulded shear strength at a given degree of remoulding. IR is equal to 0% in intact clay and to 100 % in fully remoulded conditions. Some results derived from Flon (1982) and Yong & Tang (1983) are shown in Figure 10. Results here show that as the plasticity index (I_p) of a soil increases, more energy is needed to reach fully remoulded conditions.

The remoulding energy in the test results presented by Flon (1982) and Yong & Tang (1983) are expressed with reference to the volume of the specimen. In most tests, they observed that the degree of remoulding, and thus the distribution of the remoulding energy, was non-uniform within the specimen. Since an assessment of the energy distribution was too difficult, the authors decided to define the energy per unit volume by dividing the imparted energy by the total volume of the specimen in all cases. Note that this will certainly lead to an over-estimation of the energy per unit volume.

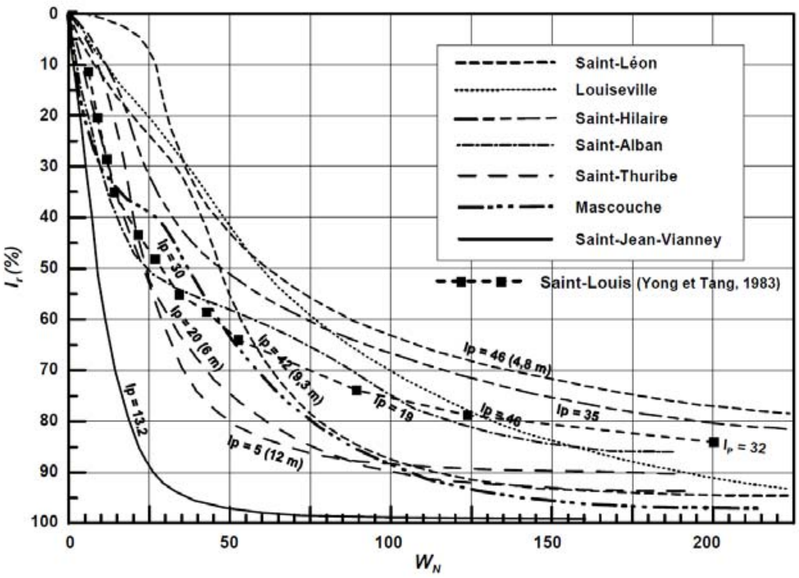

Figure 10: Curves showing the remoulding index (I_R) as a function of the normalised energy (See Eq. 10.) following the work by Flon (1982) and Yong & Tang (1983). The latter authors used the direct simple shear (DSS) apparatus from Geonor.

As mentioned above, remoulding of clay starts only after the initial peak strength has been overcome. The strain energy required to achieve this initial failure, or limit state of the clay, was investigated by Tavenas et al. (1979) who showed that the energy at the limit state for eastern Canadian clays could be expressed by reference to the preconsolidation pressure σ_p':

(7) $$W_{LS} = 0.013\ \sigma'_p$$

where W_{LS} is in kJ/m^3 (equivalent to kPa) and σ_p' in kPa. Tavenas et al. (1983) thereafter suggested expressing the remoulding energy by reference to W_{LS}, defining a normalized energy per unit volume:

(8) $$W_N = \frac{\text{Remoulded energy per unit volume}}{0.013\ \sigma'_p}$$

Based on the work by Flon (1982) and Tavenas et al. (1983), Leroueil (1996) showed that there exists a linear relationship between the product of the undrained shear strength and the plasticity index on the one side, and the average energy needed to achieve 75% of remoulding in clays on the other side (Figure 11). Locat et al. (2008) further developed this idea and showed that there is a close to linear, correlation between the remoulding index and the remoulding energy normalized by the product of s_u and I_P (Figure 12). Here the remoulding energy (E_R) was isolated from the laboratory data shown in Figure 10 by rearranging Eq. (8):

(9) $$E_R = W_N \cdot 0.013\sigma'_p$$

Looking further into Figure 12, one observes that fully remoulded conditions are achieved (i.e. I_R = 100%) when the normalized remoulding energy,

(10) $$W_N = E_R/(s_u \cdot I_P),$$

reaches a value of 16. By combining this with equations 1 and 3, the destructuration index was redefined by Locat et al. (2008) in the following way:

(11) $$I_D = \frac{\gamma \cdot H_G}{16 \cdot s_u \cdot I_p}$$

As a test, the relationship between the destructuration index and the run-out distance for Norwegian quick clay landslides is presented in Figure 13. As a first approximation here, the potential energy in the slopes was evaluated by replacing H_G in Eq. (6) by $2H/3$ (assuming undrained behavior of the clay and vertical slope). In general, results in Figure 13 show that the run-out distance increases with I_D. Landslides with an I_D value below unity show limited deformation (Lade and Frederikstad). However, for the landslides at Døla, Furre and Bekkelaget, which are also of limited deformation, the relationship between the I_D values and run-out is misleading. The I_D value calculated requires a unique value of shear strength and plasticity, which is not representative of the overall soil conditions for these three landslides. As also discussed below, the quick clay layers at Furre and Døla are very thin compared to the overlying, non-sensitive soils. The unique I_D value will therefore overestimate the run-out distance and the potential for large flow slides. A way to avoid the uniqueness problem would be to show this value in a depth profile (i.e. together with a geotechnical profile). Moreover, the relationship presented in equations 5 and 6 was acquired from laboratory data on clays from eastern Canada. These clays are generally more plastic and slightly more over-consolidated than the ones found in Norway. In order to adapt the relationships to Norwegian conditions, it is recommended to carry out a series of similar remoulding tests in the laboratory as undertaken on the Canadian clays.

In addition to the remoulded strength of the clay and the energy present in the slope, other factors such as the lateral and vertical variability of the soil deposits may control the behavior of a landslide following initial failure. To study this, the thickness of the quick clay zone (i.e. parameter *b*) is plotted against the thickness of the overlying non-sensitive soil deposits (parameter *a*) in Figure 14. The results show that the thickness of the quick clay layer must generally be equal to or larger than the overlying non-sensitive deposits for the “flow” type landslides. For these landslides, the soils on top of the quick clay zone are generally less than 5 m thick and composed of clay of low to medium sensitivity. An exception to this is the Bekkelaget landslide which did not transform into a flow slide. Here, shear strength profiles determined from vane tests show that the clay in the compression zone was less sensitive (Figure 15). The resistance met in the compression zone may have been greater than the energy available for remoulding and the slide eventually stopped.

Landslides where only limited deformation took place (i.e. spread type) are found in the lower part of Figure 14 (i.e. landslides at Døla, Frederikstad and Furre). In general, for these landslides, the thickness of the quick clay zone is small (only a few centimeters at Furre and approx. 1.5 m at Døla) and these are covered by more than 5 m of coarse and non-sensitive material (silt/sand/gravel). The landslide at Furre is interesting in this regard as even with a very thin quick clay layer, the soil body moved up to 90 m towards the river Namsen. In this example, the highly stratified soil deposits with contrasting permeability might have led to the generation of a water film (i.e. conditions of zero shear strength) as suggested in the model by Kokusho (1999).

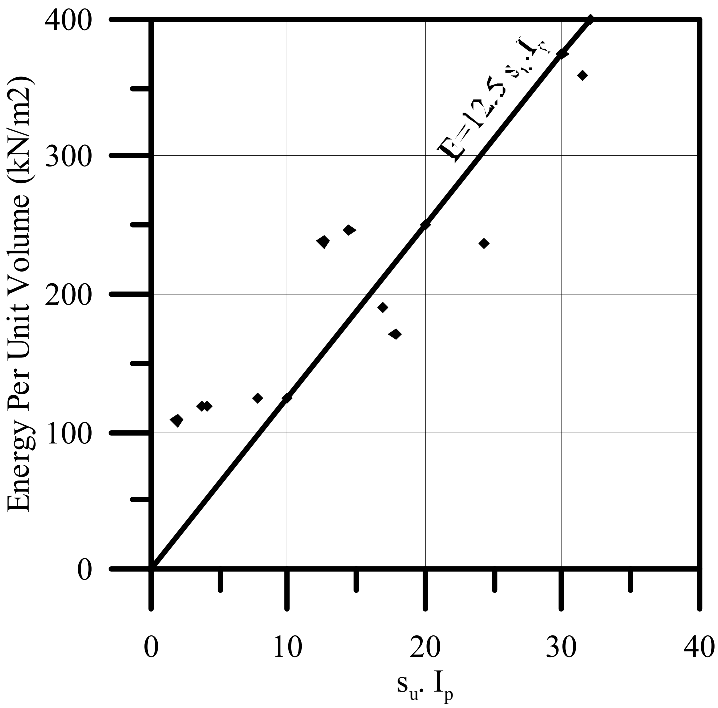

Figure 11: Energy required to achieve 75% of remoulding in soft sensitive clay at a given plasticity and undrained shear strength (from Leroueil et al. 1996).

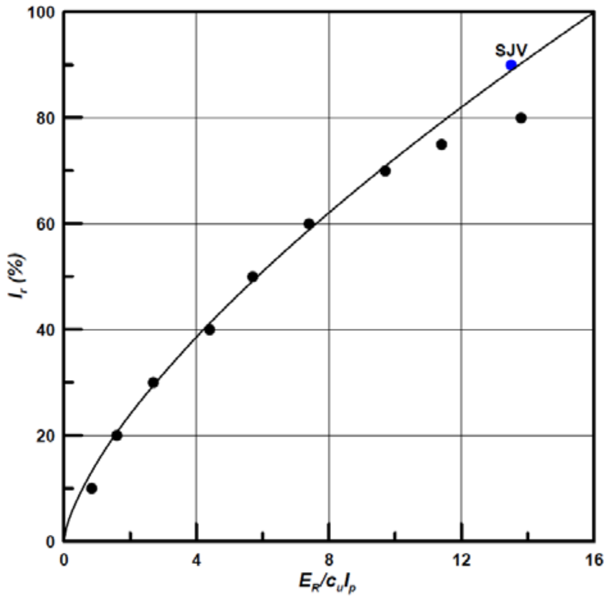

Figure 12: Relationship between the remoulding index and the remoulding energy normalized by s_u and I_p (from Locat et al. 2008). SJV is the St-Jean-Vianney landslide.

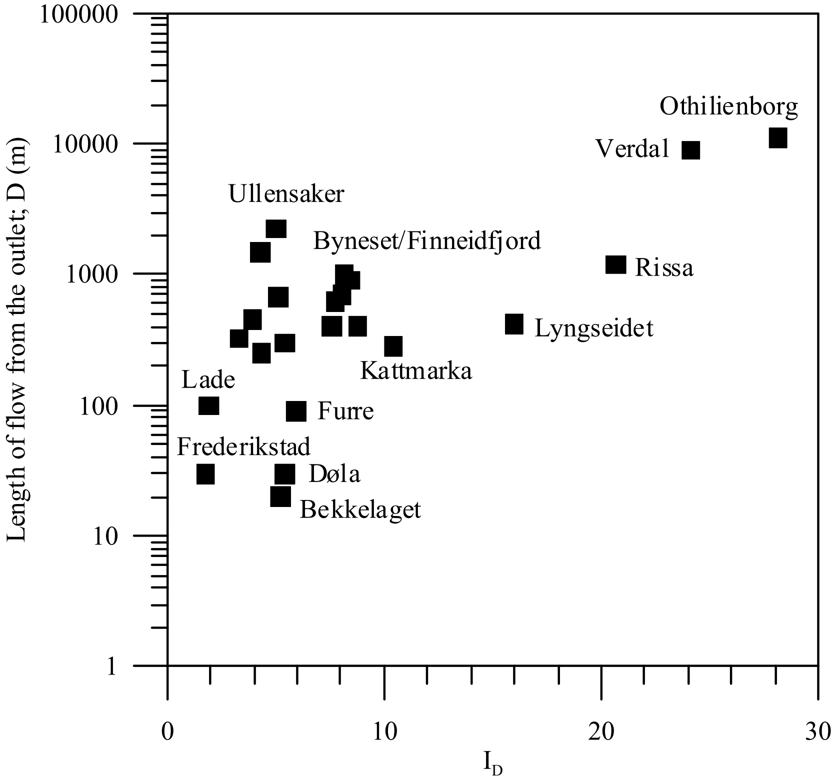

Figure 13: Relationship between the destructuration index (ID) and the run-out distance for Norwegian quick clay landslides.

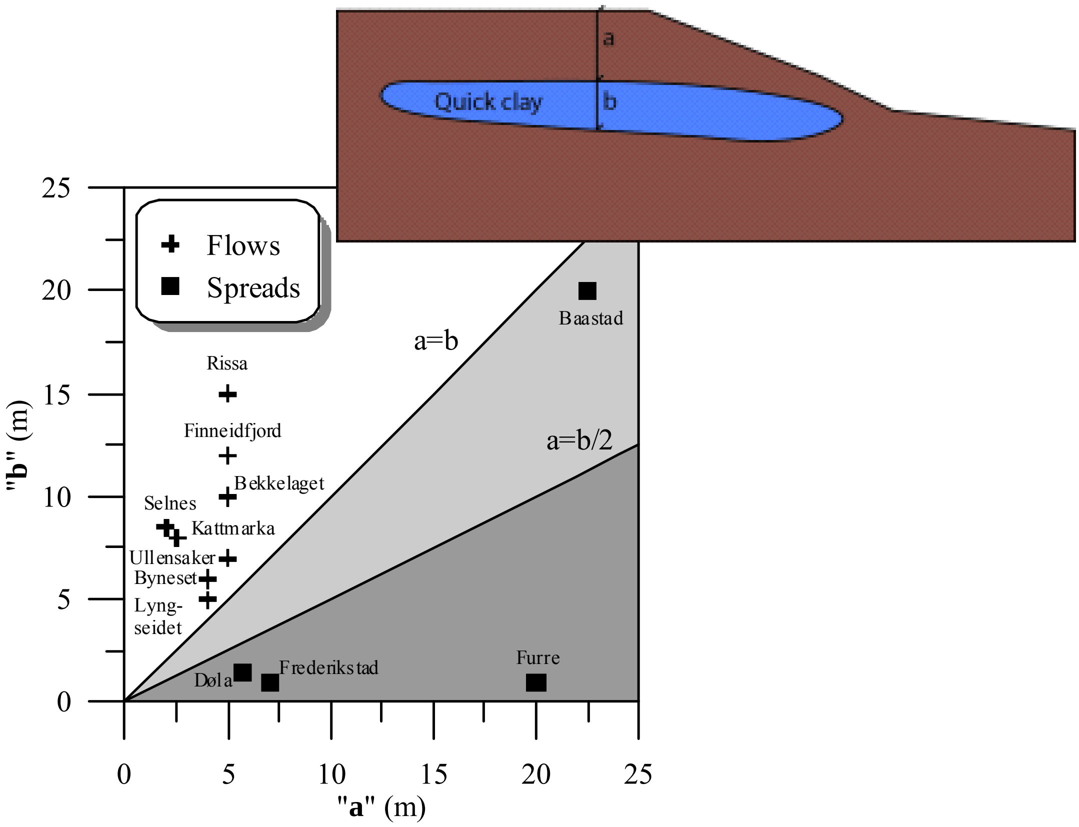

Figure 14: Impact of parameters a and b on the flow behavior and type of landslide. Parameter (a) represents the thickness of non-sensitive soil above the quick clay zone whereas parameter (b) represents the thickness of the quick clay layer.

6 Flow parameters and inputs for Q-BING

The behavior of the remoulded soil masses during the post-failure stage of a landslide must be evaluated using flow properties and rheological parameters. Edgers and Karlsrud (1982) strongly pointed out the critical role of the viscosity of the soil mass in landslide dynamics. The main types of flow are shown in Figure 16 (Couarraze and Grossiord 2000; Reiner and Scott Blair 1967), where viscosity corresponds to the slope of these curves. Thickening liquids (curve 1, Figure 16) are those for which the viscosity increases with shear rate. Shear-thinning or pseudoplastic liquids (curve 2) have an opposite behavior, as the viscosity decreases with increasing shear rate. Herschel–Bulkley fluids or Casson fluids (curve 4) are fluidizing bodies characterized by a yield stress (or yield point) and slowly decreasing viscosity at higher shear rates. Other liquid-like materials reach a constant viscosity, but only after reaching their yield-stress, are called Bingham fluids (curve 5, Figure 16).

The visco-plastic rheology governed by the Herschel-Bulkley model is given by the following relationship:

(12) $$\tau = \tau_y + K\dot{\gamma}^n \quad \text{if } |\tau| > \tau_y \quad \text{and} \quad 0 \text{ otherwise,}$$

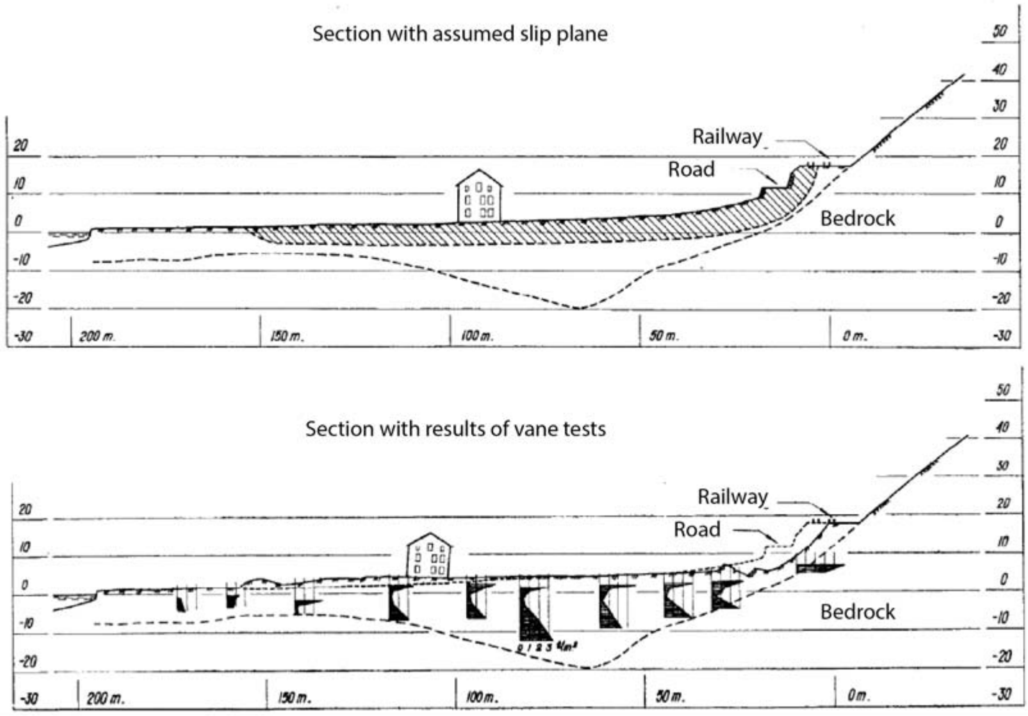

Figure 15: Section from the Bekkelaget landslide showing the terrain surface before and after the landslide. Shear strengths determined by vane tests are shown (from Eide and Bjerrum 1954).

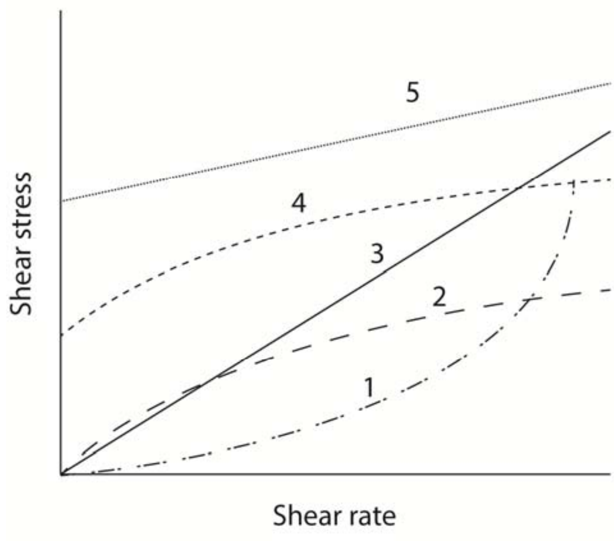

Figure 16: Major type of fluids: (1) Thickening, (2) Fluidizing or pseudoplastic, (3) Newtonian, (4) Herschel–Bulkley or Casson, (5) Bingham.

where τ is the flow resistance (kPa), τ_y is the critical yield strength (kPa), $\dot{\gamma}$ is the shear rate (s^{-1}) and n is the Herschel-Bulkley exponent (–). The parameter K—usually termed consistency—in Eq. (12) is defined as:

(13) $$K = \frac{\tau_y}{\dot{\gamma}_r^n} \quad (\text{Pa s}^n)$$

where $\dot{\gamma}_r$ is a reference strain rate (s^{-1}) defined as

(14) $$\dot{\gamma}_r = \frac{\tau_{ya}}{\mu_{dh}}$$

and where τ_{ya} is the yield strength and μ_{dh} is the plastic viscosity. Locat (1997) proposed the bilinear flow model in order to represent the rheology of clayey silt mixtures which often show pseudo-plastic flow behaviour. This model assumes that the initial phase of the flow is Newtonian and evolves, after reaching a threshold shear rate value, into a Bingham type flow. The constitutive equation for the bilinear mode is given by (Locat 1997):

(15) $$\tau = \tau_{ya} + \mu_{dh}\dot{\gamma} - \frac{\tau_{ya}\dot{\gamma}_0}{\dot{\gamma}+\dot{\gamma}_0}$$

where $\dot{\gamma}_0$ is the shear rate at the transition from a Newtonian to a Bingham behaviour. From Eq. (15) one obtains $\lim_{\dot{\gamma}\to\infty} \tau = \tau_{ya} + \mu_{dh}\dot{\gamma}$ and $\lim_{\dot{\gamma}\to 0} \tau = 0$, $\lim_{\dot{\gamma}\to 0} \frac{d\tau}{d\dot{\gamma}} = \mu_{dh} + \frac{\tau_{ya}}{\dot{\gamma}_0}$. In BING, the constitutive equation for the bilinear flow is expressed as follows (Imran et al. 2001):

(16) $$\frac{\tau}{\tau_{ya}} = 1 + \frac{\dot{\gamma}}{\dot{\gamma}_r} - \frac{1}{1+r\frac{\dot{\gamma}}{\dot{\gamma}_r}}$$

where r is the ratio of strain rates expressed as:

(17) $$r = \frac{\dot{\gamma}_r}{\dot{\gamma}_0}$$

When looking carefully at Figure 16, it becomes clear that viscosity values may change greatly with shear rate, even for a given material. For the case of sensitive clay material, however, Locat and Demers (1988) stipulated that the viscosity could be considered constant once the soil had reached its yield stress. We do not necessary agree with this when looking at some viscometer results in steady-state regime (Figure 17). Here the slope of the curves decreases significantly with increasing shear rate on the right-hand-side diagram with non-logarithmic axes, so this clay is a shear-thinning yield-stress or Casson fluid. The left-hand-side diagram shows that the shear stress increases as a low power of the shear rate.

During a landslide the flow behavior can be quite complex and various types of behavior can exist depending on the soil type and its physical characteristics. As an example, the influence of the water content on the flow behavior is shown in Figure 17. Here, an increase in water content (or I_L) leads to a reduction of the yield stress for the clay tested at a given salt content.

It is also recognized that the salt content of the clay will affect its flow behavior (Locat and Demers 1988). To study this effect, Jeong et al. (2012) performed rheological tests on illite-rich clay at the same liquidity index and with salinities varying from 0.1 to 30 g/l. The results presented in Figure 18 show that this clay exhibits a Bingham-like behavior at low salinities, but that it displays a shear-thinning behavior for increased salinity leading to an increase in the critical yield values. Results from these tests are of interest for the study of quick clay landslides in Norway as Norwegian clays also contain a considerable amount of true clay minerals, such as illite (e.g. Rosenqvist 1946). Bjerrum (1954) also showed that most Norwegian clays fall in the low-activity group (activity is the ratio of the plasticity index and clay fraction content), which is comparable to the illite-rich clay in the study by Jeong et al. (2012).

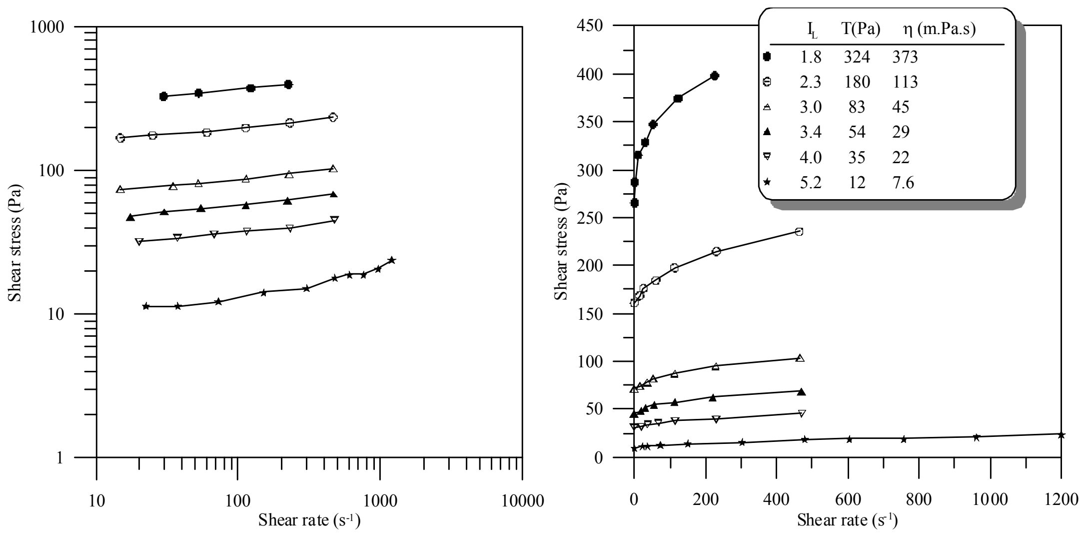

Figure 17: A series of shear rate – yield stress curves using a viscometer test on the St-Alban soil from eastern Canada. The soil was tested at various water contents and at a salt content of 0.2 g/l (T is yield stress). (Data from Locat and Demers 1988)

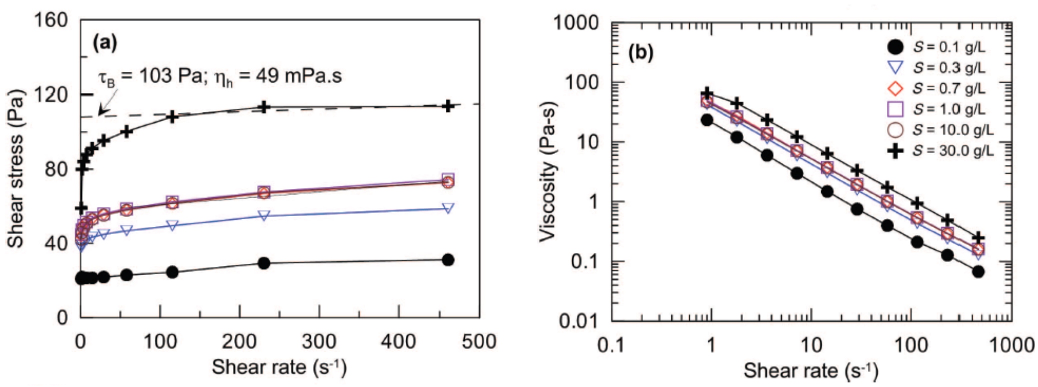

Figure 18: Flow curves of illite-rich Jonquière clay as a function of salinity (from Jeong et al. 2012).

In many situations, it may be difficult to measure the rheological behavior of a soil mixture. In Norway for example, little data is available concerning the rheological properties of sensitive clays. In order to provide estimates of yield shear strength and viscosity, results from laboratory experiments can be related to basic geotechnical index properties (e.g. the liquidity index I_L). Such correlations are possible as long as I_L is greater than 0 (i.e. for natural water content above the plastic limit). Assuming a Bingham model, Locat and Lee (2002) plotted results from plastic viscosity and yield stress measured at various liquidity indices (Figure 19). The results are partly influenced by the particle size and by the salinity in the case of the yield strength (Locat 1997). Nevertheless, for a single sediment or soil, the quality of the relationship is quite reasonable.
An interesting observation, obtained from laboratory testing, is that the yield strength contributes about 1000 times more than the viscosity to the resistance to flow of the fluid. This ratio can decrease to 100 for silty mixtures (Jeong et al. 2004). Such ratio will, however, certainly be different in the field during a landslide as the differences between the shear stresses and yield stress must be accounted for by the viscosity. Results from Figure 19 can still be used as a first approximation of the relationships between I_L and rheological parameters (see also Locat and Demers 1988, Locat 1997). For plastic viscosity (η) the relationship is of the form:

(18) $$\eta = (9.27/I_L)^{3.33}$$

where η has units of Pa·s x 10^{-3}. It is interesting to note that this relationship is based on viscometer tests performed at shear rates approximately equivalent to a velocity of 10 m/s. This is in the range observed for various landslides in sensitive clay (Table 3).

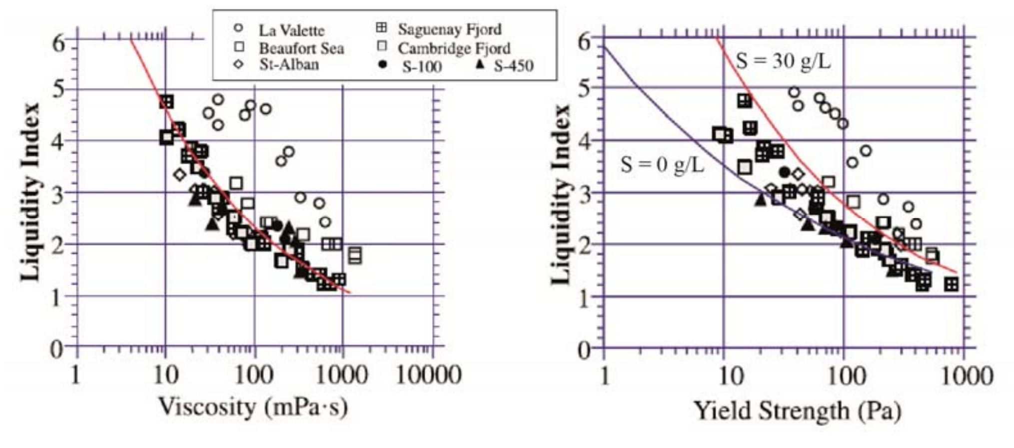

Figure 19: Relationships between the liquidity index and the rheological properties of clay soils (from Locat and Lee 2002). Note that the units of mPa·s is equivalent to Pa·s × 10^{-3}

In the case of the yield stress (τ_c), it is most clearly correlated to the liquidity index through the following two equations, one for low salinity (i.e. 0 g/l) and one for higher salinities (i.e. 30 g/l):

(19) τ_c (kPa) = 0.001 (5.81 / I_L)$^{4.55}$ for S = 0 g/l

or

(20) τ_c (kPa) = 0.001 (12.05 / I_L)$^{3.13}$ for S = 30 g/l

where S is the pore-water salinity and τ_c is in kPa. Such relationships have been successfully used to e.g. model the mobility of the giant Storegga landslide (Gauer et al. 2005), smaller slides off Vesterålen (L'Heureux et al. submitted) and the Rissa landslide (L'Heureux et al. 2012).

Another way to estimate the rheological parameters of clays is to perform back-analyses of landslide events and to study the morphology of the landslide debris. Hampton (1972) showed that the yield strength of clays during a mudflow was related to the critical flow height H_c, the buoyant unit weight of the material (γ') and the slope angle at which the flow stopped (β):

(21) $\tau_c = H_c \, \gamma' \sin \beta$

Viscous flow models have also been applied to estimate landslide velocities and to back-calculate equivalent soil viscosity given reasonable estimates of flow thickness (Figure 20; Edgers and Karlsrud 1982). Such back-analyses may, however, have limited applicability due to the rather simplified model parameters used, and uncertainties in the actual input parameters (e.g. flow thickness, slope angle and velocity).

Using the viscous flow model presented in Figure 20, Edgers and Karlsrud (1982) back-calculated soil viscosity in the range 200–400 Pa·s for the Rissa and Verdal landslides. However, based on the average liquidity index, Eq. (7) would yield viscosity values in the range 0.01 to 0.35 Pa·s. for these events and others in Norway (Table 4). This clearly illustrates the large discrepancy between laboratory and back-calculated field values of viscosity, and the need for field and laboratory calibration of these models. In the present case, the prime suspect for such a discrepancy is associated to the use of Bingham rheology on Casson fluids. At the shear rates that occur, this difference should give significant discrepancies.

Equations 8–9 were used to estimate the yield strength of Norwegian clays based on the liquidity index (Table 4). In many cases, the results are one order of magnitude lower than that estimated using the morphology of the landslide deposit (i.e. Eq. 21). However, yield strength values are closer when comparing the I_L relationship at high salinity with those from Eq. (10). The reason could be attributed to a mixing of the soil (having different pore water salinity) during the flow. In any case, results show that the remoulded shear strength in soil mechanics is similar to values of yield strength in rheology (Figure 21). This is similar to results obtained by Locat and Demers (1988) and Jeong et al. (2012).

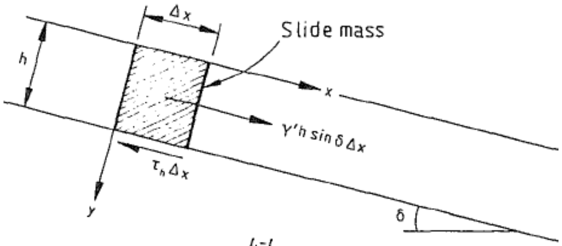

$$v = F_o + (v_i - F_o)\, e^{\frac{t_i - t}{a}}$$

$$x = x_i + F_o (t - t_i) + a (v_i - F_o) \cdot \left(1 - e^{\frac{t_i - t}{a}}\right)$$

where

$$a = \frac{(2\gamma' h \cdot \sin\delta + k)\,(\gamma' h \cdot \sin\delta - k)}{6\, g \eta\, \gamma' \sin^2\delta}$$

$$F_o = \frac{(2\gamma' h \cdot \sin\delta + k)\,(\gamma' h \cdot \sin\delta - k)^2}{(6\, \eta h \cdot \gamma \sin\delta)^2}$$

v = average flow velocity over thickness h
γ' = effective unit weight of soil
h = thickness of the flowing mass
δ = slope angle
g = acceleration of gravity
k = soil yield resistance
η = soil viscosity
t = time
$\left.\begin{array}{l} v_i \\ x_i \\ t_i \end{array}\right\}$ initial velocity, position, time

Figure 20: Summary of viscous flow analysis (from Edgers and Karlsrud 1982).

Table 4: Estimated values of flow parameters from back-analyses and empirical relationships for some Norwegian landslides.

Location	**η (Pa·s) Eq. (12)**	**η (Pa·s) (Edgers and Karlsrud 1982)**	**τ_c (kPa) (Eqs. 13-14)**	**τ_c (kPa) (Eq.15)**	**s_{ur} (kPa) Lab.**
Båstad	0.347	–	0.353-0.555	1.01	0.65
Byneset	0.013	–	0.004-0.030	0.38	0.20
Hekseberg	0.034	–	0.015-0.063	0.35	0.17
Finneidfjord	0.078	–	0.046-0.137	0.2	0.08
Rissa	0.103	200	0.068-0.178	0.36	0.24
Selnes	0.196	–	0.162-0.324	0.65	0.17
Verdal	0.078	400	0.046-0.137	–	0.2

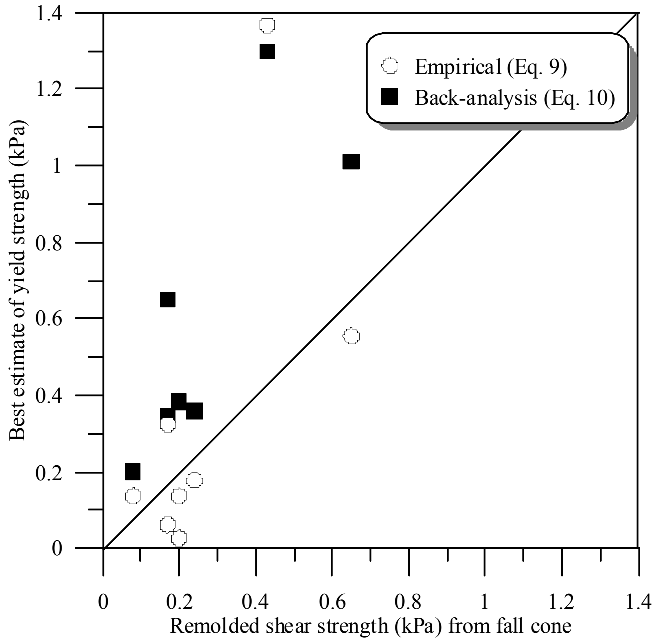

Figure 21: Comparison between remoulded shear strength values measured in the laboratory and estimates of yield strength using Eqs. 9–10.

7 Conclusions and outlook

The post-failure mechanism associated with Norwegian quick clay landslides is a complex natural phenomenon. An attempt was made in the present study to characterize the mobility of such landslides on the basis of well-documented cases and available relationships from laboratory data.

The results show that large quick clay landslides occur in Norway when the liquidity index is larger than 1.1. The data also shows that there is a link between the distance of retrogression and the mobility of landslide debris. Similarly, the mobility of quick-clay landslides increases with the mobilized volume of sediment per unit width (Vol/W_{avg}). For a given volume, the run-out distances for Norwegian landslides seem to be larger than those observed for their counterparts in eastern Canada. The reasons are attributed to the differences in mechanical properties of the clays, topography and the environment in which the landslides occur.

Following initial failure, some landslides mobilize into flows, whereas others remain as limited deformation. The reasons for this are attributed to a combination of compositional, chemical, geological and topographical factors. Lateral and vertical variations in soil profile are important agents controlling the type of landslide (i.e. flow or spread). It was shown that the susceptibility for long run-out distances could be evaluated based on relationships between the remoulding index, the destructuration index and index soil properties. In the case where the destructuration index is lower or close to unity, past landslide events have shown only limited deformation. The remoulding and flow parameters presented in this report are mostly based on data from eastern Canada where the clays are generally more plastic and more over-consolidated and with higher normalized undrained strength than the ones found in Norway. It is therefore in the future recommended to carry out similar viscosity and remoulding tests on Norwegian clay as have been undertaken and reported for Canadian clays.

During a landslide event the flow behavior can be quite complex and various types of flow behavior can exist depending on the soil type, pore-water salinity, mineralogy, and water content. Results show that the remoulded shear strength in soil mechanics is similar to values of yield strength in rheology. There is, however, a large discrepancy between the values of viscosity determined directly from laboratory data and those obtained empirically from back-calculation of landslide events. There is therefore a need for field and laboratory calibration of these models or, alternatively, for models that predict changes in the material properties of the sliding materials due to shearing and water ingestion.

8 References

Aas, G. 1981. Stability of natural slopes in quick clays, In Proceedings of the tenth International Conference on Soil Mechanics and Foundation Engineering, Stockholm. Sweden, 15-19 June 1981. Norwegian Geotechnical Institute, Oslo, Norway. Publication no. 135, pp. 333–338.

Bjerrum, L., 1954. Geotechnical properties of Norwegian marine clays. Géotechnique, 4(2): 49–69.

Bjerrum, L. 1955. Stability of natural slopes in quick clay. Géotechnique, 5: 101–119.

Bjerrum L. & Kjærnsli B. 1957. Analysis of the stability of some Norwegian natural clay slopes. Geotechnique, 7: 1–16.

Callander, P.F. et Smalley, I.J. 1984. An application of Soderblom's rapidity test to Canadian soils. Engineering Geology, 20 (3): 235–240.

Couarraze, G., & Grossiord, J.-L., 2000. Initiation à la rhéologie. Lavoisier, Paris, France. 3rd ed., TEC & DOC (Editions)

Cruden, D. M. & Varnes D. J. 1996. Landslides types and processes. In Landslides investigation and mitigation, Special Report 247, Transportation, Research Board, National Research Council, *Edited by* A. K. Turner, and R. L. Schuster, National Academy press, Washington, D.C. pp. 37–75.

Drury, P. 1968. The Hekseberg landslide, March 1967. NGI publication, No. 75, pp. 27–31.

Eide, O. & Bjerrum, L. 1955. The slide at Bekkelaget." Geotechnique, 5: 88-100.

Edgers, L., & Karlsrud, K., 1982: Soil flows generated by submarine slides - Case studies and consequences. International Conference on the Behavior of Off-Shore Structures, 3. BOSS'82. Cambridge, Mass 1982. Proceedings, Vol. 2, pp. 425–437.

Flon, P. 1982. Remoulding energy and retrogression during flowslides. Master thesis (MSc.), Département de génie civil, Université Laval, Québec, Canada, 292 pp.

Furseth, A. 2006: Skredulykker i Norge. Tun Forlag, Oslo.

Gauer, P., Kvalstad, T. J., Forsberg, C. F., Bryn, P., & Berg, K. 2005. The last phase of the Storegga Slide: Simulation of retrogressive slide dynamics and comparison with slide-scar morphology, Mar. Petrol. Geol., 22: 171–178.

Geertsema, M., Cruden, D. M., Schwab, J. W. 2006. A large landslide in sensitive glaciomarine sediments at Mink Creek, northwestern British Columbia, Canada. Engineering Geology, 83(1–3): 36–63.

Gregersen, O. 1981. The Quick Clay Landslide in Rissa, Norway. Contribution to the Tenth International Conference on Soil Mechanics and Foundation Engineering, Stockholm, Sweden, 15-19 June 1981. Norwegian Geotechnical Institute, Oslo, Norway. Publication No. 135. pp. 421–426.

Gregersen, O. & Løken T. 1979. The quick-clay slide at Baastad, Norway, 1974. Engineering Geology, 14: 183–196.

Hansen, L., L'Heureux, J.S., Longva, O. & Eilertsen, R.S. 2011 Undersjøiske landformer og skredprosesser langs strandsonen i Drammensfjorden. NGU Rapport 2011.003.

Holmsen, G. 1929. Lerfaldene ved Kokstad, Gretnes og Braa. Norges Geol. Unders. 132, 45 pp. (In Norwegian)

Holmsen, G. & Holmsen, P. 1946. Leirfall i årene 1940–1945. Norges Geol. Unders. 167, 71 pp. (In Norwegian)

Hutchinson, D.J. 1961. A landslide on a thin layer of quick clay at Furre, central Norway. Geotechnique, 11: 69–94.

Hutchinson, J.N. 1965. The landslide of February, 1959, at Vibstad in Namdalen. Norwegian Geotechnical Institute. Publ. 61: 1–16.

Ilstad, T., De Blasio F.V., Elverhoi, A., Harbitz, C.B., Engvik, L., Longva, O. & Marr, J.G. 2004: On the frontal dynamics and morphology of submarine debris flows. Marine Geology, 213: 481–497.

Imran, J., Parker, G., Locat, J., Lee, H., 2001. A 1-D numerical model of muddy subaqueous and subaerial debris flows. J. Hydraul. Eng. 127, 959–968.

Jeong, S.W., Locat, J., & Leroueil, S., 2004: A preliminary analysis of the rheological transformation due to water infiltration as a mechanism for high mobility of submarine mass movements. Proceedings of the 57th Canadian Geotechnical Conference, Quebec city, pp. 15–22.

Jeong, S.W., Locat, J., Leroueil, S., 2012: The effect of salinity and shear history on the rheological characteristics of illite-rich and Na-Montmorillonite-rich clays. Clays and Clay Minerals, 60(2): 108–120.

Karlsrud, K. 1979. Skredfare og planlegging. Forelesningsnoter til NIF-kurs. Norske sivilingeniørers forening i samarbeid med Norges geotekniske institutt. Lofthus, Hardanger. (In Norwegian)

Karlsrud, K. & By, T. 1981. Data on Run-Out Distance and Velocity of Soil Flows Generated by Subaqueous Slides and Quick-Clay Slides. Norwegian Geotechnical Institute, Report 52207-7.

Karlsrud, K. 1983. Analysis of a small slide in sensitive clay in Frederikstad, Norway. Proceedings of the symposium on slopes in soft clay; Linköping, Sweden. SGI report no 17, pp. 175–184.

Karlsrud, K., Aas, G. & Gregersen, O. 1984. Can we predict landslide hazards in soft sensitive clays? Summary of Norwegian practice and experiences. In Proceedings of the 4th International Symposium on Landslides, Toronto, Ont., 16–21 September 1984. University of Toronto Press, Toronto, Ont. Volume 1, pp. 107–130.

Karlsrud, K., & Hernadez-Martinez, F.G. 2012. Strength and deformation properties of Norwegian clays from laboratory tests on high quality block samples. Manuscript submitted to the Canadian Geotechnical Journal.

Kenney, T.C. 1967. Slide behaviour and shear resistance of a quick clay determined from a study of the landslide at Selnes, Norway. NGI publ. 76: 57-64.

Kokusho, T., 1999: Water film in liquefied sand and its effect on lateral spread. Journal of Geotechnical and Geoenvironmental Engineering, 125(10): 817–826.

Lebuis, J., Robert, J.-M., & Rissmann, P. 1983. Regional mapping of landslide hazard in Québec. Symposium on slopes on soft clays, Linkoping, Swedish Geotechnical Institute Report, No. 17: 205–262.

Leroueil, S., Vaunat, J., Picarelli, L., Locat, J., Faure, R. & Lee, H. 1996. A geotechnical characterisation of slope movements. In: Proceedings of the 7th symposium on landslides, Trondheim, vol. 1, pp. 53–74.

L'Heureux, J.-S., Hansen, L., & Longva, O. 2009. Development of the submarine channel in front of the Nidelva River, Trondheimsfjorden, Norway. Marine Geology, 260: 30–44.

L'Heureux, J.S., Eilertsen, R.S., Hansen, L. & Sletten, K. 2011. Morphology and landslide mapping in lake Botnen at Rissa, Sør Trøndelag. NGU Rapport 2011.037. (In Norwegian)

L'Heureux, J.S. 2012. A study of the retrogressive behavior and mobility of Norwegian quick clay landslides. Proceedings of the 11th International & 2nd North American Symposium on Landslides, Banff, Canada.

L'Heureux, J.S., Eilertsen, R.S., Glimstad, S., Issler, D., Solberg, I.-L., & Harbitz, C.B. 2012. The 1978 quick clay landslide at Rissa, mid-Norway: subaqueous morphology and tsunami simulations. In: Y. Yamada et al. (eds.), Submarine Mass Movements and Their Consequences, Advances in Natural and Technological Hazards Research 31, Springer Science+Business Media B.V. DOI 10.1007/978-94-007-2162-3_45.

L'Heureux, J.S., & Solberg, I.L. 2012. Utstrekning og utløpsdistanse for kvikkleireskred basert på katalog over skredhendelser i Norge. NGU rapport nr. 2012.040.

L'Heureux, J.S., Vanneste, M., Rise, L., Brendryen, J., Forsberg, C.F., Nadim, F., Longva, O., Chand, S., Kvalstad, T.J., & Haflidason, H., (submitted). Stability, mobility and failure mechanism for landslides at the Upper Continental Slope off Vesterålen, Norway. Marine Geology.

Longva, O., Janbu, N., Blikra, L.H. & Boe R. (2003) The 1996 Finneidfjord slide: seafloor failure and slide dynamics. In: Locat J, Mienert J (eds) Submarine mass movements and their consequences. Kluwer Academic, Dordrecht, pp. 531–538.

Locat, A., Leroueil, S., Bernander, S., Demers, D., Jostad, H. P. & Ouehb, L. 2011. Progressive failures in Eastern Canadian and Scandinavian sensitive clays. Canadian Geotechnical Journal, 48(11): 1696–1712.

Locat, J., & Demers, D., 1988. Viscosity, yield stress, remoulded strength and liquidity index relatiosnhips for sensitive clays. Canadian Geotechnical Journal, 25: 799–806.

Locat, J., & Leroueil, S. 1997. Landslide stages and risk assessment issues in sensitive clays and other soft sediments. *In:* Cruden & Fell (Eds.) Landslide risk assessment, Balkema, Rotterdam, pp. 261–270.

Locat, J. 1992. Viscosity, yield strength, and mudflow mobility for sensitive clays and other fine sediments. Proceedings of the 1st Canadian conference on Geotechnique and Natural Hazards, Vancouver, pp.: 389-396.

Locat, J., & Lee, H.J. 2002. Submarine landslides: advances and challenges. Canadian Geotechnical Journal, 39:193–212.

Locat, J., Leroueil, S., et Locat, P. 2003. On the mobility of quick clays: the cases of the St. Jean-Vianney Flowslides of 1663 and 1971. In: Proceedings of the International Work-shop on Occurrence and Mechanisms of Flow-like Land-slides in Natural Slopes and Earthfills, Sorrento.

Locat, P., Leroueil, S. & Locat, J. 2008: Remaniement et mobilité des débris de glissements de terrain dans les argiles sensibles de l'est du Canada. Proceedings of the 4th Canadian Conference on Geohazards: From Causes to Management. Presse de l'Université Laval, Québec, pp. 97–106. (In French)

Locat, P., Fournier, T., Robitaille, D., & Locat, A. 2011. Glissement de terrain du 10 mai 2010, St-Jude, Montérégie. Rapport sur les caractéristiques et les causes. Ministères des Transports du Québec, report MT11-01. (In French)

Longva, O., Janbu, N., Blikra, L.H. & Boe R. (2003) The 1996 Finneidfjord slide: seafloor failure and slide dynamics. In: Locat, J., & Mienert. J. (eds.), Submarine mass movements and their consequences. Kluwer Academic, Dordrecht, pp. 531–538.

Løken, T. 1983: Kvikkleire og skredfare – hvor og hvorfor? Forskningsnytt fra Norges almenvitenskapelige forskningsråd, 28(3): 7–12.

Mitchell, R.J., & Markell, A.R. 1974. Flowslides in sensitive soils. Canadian Geotechnical Journal, 11: 11–31.

Natterøy, A. 2011: Skredkatalog om kvikkleire. Presentasjon av det førebels resultatet i katalogen og utgreiing om typiske kjennetegn ved kvikkleireskred. Prosjektoppgave. Institutt for geologi og bergteknikk, NTNU. (In Norwegian)

NGI (2011). Leirskred Døla, Mosjøen. Rapport nr. 2011.0544

Norges vassdrags- og energidirektorat (NVE) 2009: Retningsliner for planlegging og utbygging i fareområder langs vassdrag. Retningslinjer nr. 1/2008 (rev. 05.03. 2009).

Nordal, S., Alén, C., Emdal, A., Jendeby, L., Lyche, E., & Madshus, C. 2009. Skredet i Kattmarkvegen i Namsos 13. mars 2009. Rapport fra undersøkelsesgruppe satt ned av Samferdselsdepartementet. Institutt for bygg, anlegg og transport, faggruppe for geoteknikk, NTNU. (In Norwegian)

Norges vassdrags- og energidirektorat (NVE) 2009: Retningsliner for planlegging og utbygging i fareområder langs vassdrag. Retningslinjer nr. 1/2008 (rev. 05.03. 2009). (In Norwegian)

Norsk Geoteknisk Forening (NGF) 1974: Retningslinjer for presentasjon av geotekniske undersøkelser. 16 pp. (In Norwegian)

Reiner, M., & Scott Blair, G.W. 1967. Rheological terminology. *In* Rheology: theory and applications. Vol. 4. Edited by F. R. Eirich. Academic Press, New York, NY, pp. 461–488.

Rokoengen, K., Jespersen, M. N., Kleiv, R. A. & Sæterbø, E. 2001. The 1345 slide and flood disaster in the Gauldalen valley, Mid-Norway: a new interpretation. Norwegian Journal of Geography, 55: 57–70.

Rosenqvist, I.T., 1946. Om de norske kvikkleirers egenskaper og mineralogiske sammensetning. 3: E. Nordiska Ingeniørmøtet Förhandlingar 10 : 1. Stockholm. (In Norwegian)

Rosenqvist, I.T. 1953. Considerations on the sensitivity of Norwegian clays. Geotechnique, 3: 195–200.

Rosenqvist, I.T. 1966. The Norwegian Research into the development of quick clay – a review. Engineering Geology, 1: 445-450.

Söderblom, R. 1974. A new approach of the classification of quick clays. SGI, Proc. No. 55, pp. 1–17.

Sevaldson, R.A. 1956. The slide in Lodalen, October 6th, 1954, Geotechnique, 6: 167–182.

Tavenas, F., Chagnon, J.-Y. & La Rochelle, P. 1971. The Saint-Jean-Vianney landslide: Observations and eyewitness accounts. Canadian Geotechnical Journal, 8: 463–478.

Tavenas, F., Desrosiers, J.P., Leroueil, S., LaRochelle, P., & Roy, M. 1979. The use of strain energy as a yield and creep criterion for lightly overconsolidated clays. Géotechnique, 29(3): 285–303.

Tavenas, F., Flon, P., Leroueil, S. & Lebuis, J. 1983. Remoulding energy and risk of slide retrogression in sensitive clays. In: Proceedings of the Symposium on slopes on soft clays, Linköping, Sweden. Swedish Geotechnical Institute, SGI Report No. 17, pp. 423–454.

Tavenas, F. 1984. Landslides in Canadian sensitive clays - a state-of-the-art. *In* Proceedings of the 4th International Symposium on Landslides, Toronto, Ont., 16–21 September 1984. University of Toronto Press, Toronto, Ont. Volume 1, pp. 141–153.

Thakur, V., and Degago, S.A. (2012) Quickness of sensitive clays. Géotechnique Letters 2, 81–88.

Trak B. & Lacasse S. 1996. Soils susceptible to flow slides and associated mechanisms. In: Proceedings of the Seventh International Symposium on Landslides, Trondheim, Norway, Balkema, Rotterdam, Vol. 1, pp. 497–506.

Vaunat, J. 2002. Contributions à l'élaboration d'un système à base de connaissance pour la prévision des risques liés aux mouvements de terrains. PhD thesis, Département de génie civil, Université Laval, Canada. (In French)

Vaunat, J., & Leroueil, S. 2002. Analysis of post-failure slope movements within the framework of hazard and risk analysis. Natural Hazards, 26: 83–109.

Walberg, Ø. 1993: Verdalsboka. Ras i Verdal, vol A and B. Verdal kommune, Norway. (In Norwegian)

Yong, R. N., & Tang, K.Y. 1983. Soil remoulding and sensitivity measurements. Geotechnical Testing Journal, 6(2): 73–80.

Kontroll- og referanseside/
Review and reference page

NGI

Dokumentinformasjon/*Document information*		
Dokumenttittel/*Document title* Characterization of historical quick clay landslides and input parameters for Q-Bing		**Dokument nr./*Document No.*** 20120753-02-R
Dokumenttype/*Type of document* Report	**Distribusjon/*Distribution*** Unlimited	**Dato/*Date*** 17 January 2013 **Rev.nr.&dato/*Rev.No&date.*** 0
Oppdragsgiver/*Client* Statens Vegvesen, Vegdirektoratet v/Vikas Thakur		
Emneord/*Keywords* Quick-clay slides, rheology, historical events, geotechnical parameters		

Stedfesting/*Geographical information*	
Land, fylke/*Country, County* —	**Havområde/*Offshore area***
Kommune/*Municipality* —	**Feltnavn/*Field name***
Sted/*Location* —	**Sted/*Location***
Kartblad/*Map* —	**Felt, blokknr./*Field, Block No.***
UTM-koordinater/*UTM-coordinates* —	

Dokumentkontroll/*Document control*

Kvalitetssikring i henhold til/*Quality assurance according to* NS-EN ISO9001

Rev./ *Rev.*	**Revisjonsgrunnlag/*Reason for revision***	**Egen-kontroll/ *Self review* av/*by:***	**Sidemanns-kontroll/ *Colleague review* av/*by:***	**Uavhengig kontroll/ *Independent review* av/*by:***	**Tverrfaglig kontroll/ *Inter-disciplinary review* av/*by:***
0	Original document	JSL	KK	DI	

Dokument godkjent for utsendelse/ *Document approved for release*	**Dato/*Date*** 17 January 2013	**Sign. Prosjektleder/*Project Manager*** Dieter Issler

NGI (Norges Geotekniske Institutt) er et internasjonalt ledende senter for forskning og rådgivning innen geofagene. Vi utvikler optimale løsninger for samfunnet, og tilbyr ekspertise om jord, berg og snø og deres påvirkning på miljøet, konstruksjoner og anlegg.

Vi arbeider i følgende markeder: olje,gass og energi, bygg, anlegg og samferdsel, naturskade og miljøteknologi. NGI er en privat stiftelse med kontor og laboratorier i Oslo, avdelingskontor i Trondheim og datterselskap i Houston, Texas, USA.

NGI ble utnevnt til "Senter for fremragende forskning" (SFF) i 2002 og leder "International Centre for Geohazards" (ICG).

www.ngi.no

NGI (Norwegian Geotechnical Institute) is a leading international centre for research and consulting in the geosciences. NGI develops optimum solutions for society, and offers expertise on the behaviour of soil, rock and snow and their interaction with the natural and built environment.

NGI works within the oil, gas and energy, building and construction, transportation, natural hazards and environment sectors. NGI is a private foundation with office and laboratory in Oslo, branch office in Trondheim and daughter company in Houston, Texas, USA.

NGI was awarded Centre of Excellence status in 2002 and leads the International Centre for Geohazards (ICG).

www.ngi.no

Hovedkontor/Main office:
PO Box 3930 Ullevål Stadion
NO-0806 Oslo
Norway

Besøksadresse/Street address:
Sognsveien 72, NO-0855 Oslo

Avd Trondheim/Trondheim office:
PO Box 1230 Sluppen
NO-7462 Trondheim
Norway

Besøksadresse/Street address:
Pirsenteret, Havnegata 9, NO-7010 Trondheim

T: (+47) 22 02 30 00
F: (+47) 22 23 04 48

ngi@ngi.no
www.ngi.no

Kontonr 5096 05 01281/IBAN NO26 5096 0501 281
Org. nr/Company No.: 958 254 318 MVA

BSI EN ISO 9001
Sertifisert av/Certified by BSI, Reg. No. FS 32989

Denne serien utgis av Norges vassdrags- og energidirektorat (NVE)

Utgitt i Rapportserien i 2013

Nr. 1 Roller i det nasjonale arbeidet med håndtering av naturfarer for tre samarbeidende direktorat
Nr. 2 Norwegian Hydrological Reference Dataset for Climate Change Studies. Anne K. Fleig (Ed.)
Nr. 3 Anlegging av regnbed. En billedkavalkade over 4 anlagte regnbed
Nr. 4 Faresonekart skred Odda kommune
Nr. 5 Faresonekart skred Årdal kommune
Nr. 6 Sammenfatning av planlagte investeringer i sentral- og regionalnettet for perioden 2012-2021
Nr. 7 Vandringshindere i Gaula, Namsen og Stjørdalselva
Nr. 8 Kvartalsrapport for kraftmarknaden. Ellen Skaansar (red.)
Nr. 9 Energibruk i kontorbygg – trender og drivere
Nr. 10 Flomsonekart Delprosjekt Levanger. Kjartan Orvedal, Julio Pereira
Nr. 11 Årsrapport for tilsyn 2012
Nr. 12 Report from field trip, Ethiopia. Preparation for ADCP testing (14-21.08.2012)
Nr. 13 Vindkraft - produksjon i 2012
Nr. 14 Statistikk over nettleie i regional- og distribusjonsnettet 2013. Inger Sætrang
Nr. 15 Klimatilpasning i energiforsyningen- status 2012. Hvor står vi nå?
Nr. 16 Energy consumption 2012. Household energy consumption
Nr. 17 Bioenergipotensialet i industrielt avfall
Nr. 18 Utvikling i nøkkeltall for strømnettselskapene
Nr. 19 NVEs årsmelding
Nr. 20 Oversikt over vedtak og utvalgte saker. Tariffer og vilkår for overføring av kraft i 2012
Nr. 21 Naturfareprosjektet: Delprosjekt Kvikkleire. Utstrekning og utløpsdistanse for kvikkleireskred basert på katalog over skredhendelser i Norge
Nr. 22 Naturfareprosjektet: Delprosjekt Kvikkleire. Forebyggende kartlegging mot skred langs strandsonen i Norge Oppsummering av erfaring og anbefalinger
Nr. 23 Naturfareprosjektet: Delprosjekt Kvikkleire. Nasjonal database for grunnundersøkelser (NADAG) – forundersøkelse
Nr. 24 Flom og skred i Troms juli 2012. Inger Karin Engen, Graziella Devoli, Knut A. Hoseth, Lars-Evan Pettersson
Nr. 25 Capacity Building in Hydrological Services. ADCP and Pressure Sensor Training Ministry of Water and Energy, Ethiopia 20th – 28th February 2013
Nr. 26 Naturfareprosjektet: Delprosjekt Kvikkleire. Vurdering av kartleggingsgrunnlaget for kvikkleire i strandsonen
Nr. 27 Kvartalsrapport for kraftmarknaden. Ellen Skaansar (red.)
Nr. 28 Flomberegninger for Fedaelva, Kvinesdal kommune, Vest-Agder (025.3A1) Per Alve Glad
Nr. 29 Beregning av energitilsig basert på HBV-modeller. Erik Holmquist
Nr. 30 De ustabile fjellsidene i Stampa – Flåm, Aurland kommune Sammenstilling, scenario, risiko og anbefalinger. Lars Harald Blikra
Nr. 31 Naturfareprosjektet: Delprosjekt 4 Overvåking og varsling Overvåking ved akutte skredhendelser
Nr. 32 Landsomfattende mark- og grunnvannsnett. Drift og formidling 2012. Jonatan Haga
Nr. 33 Naturfareprosjektet: Delprosjekt 6 Kvikkleire. Saltdiffusjon som grunnforsterking i kvikkleire
Nr. 34 Kostnadseffektivitet i distribusjonsnettet – En studie av referentene i kostnadsnormmodellen
Nr. 35 The unstable phyllitic rocks in Stampa – Flåm, western Norway Compilation, scenarios, risk and recommendations. Lars Harald Blikra
Nr. 36 Flaumsonekart Delprosjekt Årdal i Sogn. Siss-May Edvardsen, Camilla Roald
Nr. 37 Naturfareprosjektet: Delprosjekt 6 Kvikkleire. Skånsomme installasjonsmetoder for kalksementpeler og bruk av slurry
Nr. 38 Naturfareprosjektet: Delprosjekt 6 Kvikkleire. Karakterisering av historiske kvikkleireskred og input parametere for Q-BING
Nr. 39 Naturfareprosjektet: Delprosjekt 6 Kvikkleire. Natural Hazards project: Work Package 6 - Quick clay Characterization of historical quick clay landslides and input parameters for Q-Bing

Norges
vassdrags- og
energidirektorat

N V E

Norges vassdrags- og energidirektorat

Middelthunsgate 29
Postboks 5091 Majorstuen
0301 Oslo

Telefon: 09575
Internett: www.nve.no